# Extension of the Total Carbon Column Observing Network (TCCON) over the Eastern Mediterranean and Middle East: The Nicosia site in Cyprus

Constantina Rousogenous[1], Christof Petri[2], Pierre-Yves Quéhé[1], Thomas Laemmel[3,a], Joshua L. Laughner[4], Maximilien Desservettaz[1,b], Michael Pikridas[1], Michel Ramonet[3], Efstratios Bourtsoukidis[1], Matthias Buschmann[2], Justus Notholt[2], Thorsten Warneke[2], Jean-Daniel Paris[3,1], Jean Sciare[1] and Mihalis Vrekoussis[2,1,5]

[1]Climate and Atmosphere Research Centre (CARE-C), The Cyprus Institute, Nicosia, 2121, Cyprus
[2]Institute of Environmental Physics (IUP), University of Bremen, Bremen, 28359, Germany
[3]Laboratoire des Sciences du Climat et de l'Environnement (LSCE/IPSL), Université Paris-Saclay, CEA, CNRS, UVSQ, Gif-sur-Yvette, 91191, France
[4]Jet Propulsion Laboratory, California Institute of Technology, Pasadena, CA, 91109, USA
[5]Center of Marine Environmental Sciences (MARUM), University of Bremen, Bremen, 28359, Germany
[a]now at: University of Bern, Department of Chemistry, Biochemistry and Pharmaceutical Sciences and Oeschger Center for Climate Change Research, Bern, Switzerland
[b]now at: Environmental Futures, School of Science, University of Wollongong, Wollongong, New South Wales, Australia

Correspondence to: Constantina Rousogenous (c.rousogenous@cyi.ac.cy)

**Abstract.** Long-term greenhouse gas (GHG) measurements are essential for understanding the carbon cycle, detecting trends in atmospheric composition, and assessing the efficiency of climate change mitigation strategies. However, observational gaps over large geographic areas such as the Eastern Mediterranean and Middle East (EMME), a well-known regional GHG hotspot, are likely to increase uncertainties in estimations of their sources and sinks. Here, we describe a new Total Carbon Column Observing Network (TCCON) observatory for solar absorption spectroscopy measurements that has been operating in Nicosia, Cyprus, since September 2019. The site helps bridge a regional observational gap in the EMME, a strategic location at the crossroads of air masses from Europe, Asia, and Africa. Using near-infrared (NIR, InGaAs detector) solar absorption spectra, TCCON-Nicosia measures total column average dry-air mole fractions ($X_{gas}$) of key trace gases, including carbon dioxide ($CO_2$), methane ($CH_4$), nitrous oxide ($N_2O$), carbon monoxide (CO), hydrogen fluoride (HF), water vapor ($H_2O$), and semi-heavy water (HDO). These continuous observations, spanning more than four years, are presented along with a description of the quality control procedures, compliant with the TCCON standards, to ensure total column atmospheric data with minimal errors.

In 2023, observations were extended into the mid-infrared (MIR) spectral region with the addition of a liquid-nitrogen-cooled InSb ($LN_2$-InSb) detector enabling the retrieval of additional trace gases such as formaldehyde (HCHO), carbonyl sulfide (OCS), nitrogen monoxide (NO), nitrogen dioxide ($NO_2$), and ethane ($C_2H_6$), herewith further contributing to the global Network for the Detection of Atmospheric Composition Change (NDACC).

Deleted: spectrum

To tie the TCCON Nicosia with the WMO reference scale, an AirCore (AC) campaign conducted in June 2020 over Cyprus provided vertical in situ profiles, which were converted into total column quantities ($AC.X_{gas}$) and compared to TCCON observations ($X_{gas}$). The TCCON/in situ comparison showed agreement well within their respective uncertainty budget.

Deleted: error

## 1 Introduction

Efforts to reduce greenhouse gas (GHG) emissions are crucial for mitigating climate change. In this context, observational networks play a key role in monitoring the spatial and temporal variations of these gases in the atmosphere (Ciais et al., 2014), providing valuable data for inferring sources and sinks and therefore, enhancing global GHG reporting (Deng et al., 2022).

The Total Carbon Column Observing Network (TCCON, Wunch et al., 2011), is a spatially sparse network of high-resolution Fourier transform spectrometers (FTS), measuring in the near-infrared (NIR) region. It is designed to provide long-term (multi-year), accurate and precise retrievals of several atmospheric trace gases, including carbon dioxide ($CO_2$), methane ($CH_4$), nitrous oxide ($N_2O$), water vapor ($H_2O$), semi-heavy water (HDO), hydrofluoric acid (HF) and carbon monoxide (CO) (Wunch et al., 2011). TCCON data products are column-averaged dry-air mole fractions (DMFs) of these gases, denoted as $X_{gas}$. TCCON columnar observations are widely used to estimate GHG fluxes (Fraser et al., 2013; Keppel-Aleks et al., 2012), assess urban GHG emissions (Babenhauserheide et al., 2020; Hedelius et al., 2017), and serve as reference values for satellite validation and model evaluation (Byrne et al., 2023; Sha et al., 2021).

Although crucial for atmospheric monitoring, the TCCON network, with currently 29 operational sites, has large spatial gaps, particularly across large regions such as Africa, Central and West Asia, Siberia, the Mediterranean and Middle East region, and South America (https://tccondata.org/, last access: 1 March 2025). These gaps limit the comprehensive validation of satellite measurements and the evaluation of model simulations which are essential for inferring global GHG fluxes with reduced uncertainty (Bastos et al., 2020; Schimel et al., 2015). To address this, a new TCCON site was established in September 2019 in Cyprus, aimed at filling the observational gap in the Eastern Mediterranean and Middle East (EMME) region (Fig.1a).

Cyprus (Fig. 1b) is the third largest and most eastern Mediterranean island, with low local GHG emissions, raking 24th in EU27 with a total emissions share of 0.3 % in 2022 (https://www.eea.europa.eu/en/analysis/publications/annual-european-union-greenhouse-gas-inventory, last access: 1 March 2025). Furthermore, previous studies have shown that long-range transported pollution dominates over local emissions in Cyprus, with distinct seasonal air-mass regimes originating from Europe, west Asia (including the Middle East), and North Africa (Kleanthous et al., 2014; Lelieveld et al., 2002; Pikridas et al., 2018; Vrekoussis et al., 2022; Germain-Piaulenne et al., 2024). This diversity of source regions; regions which currently exhibit diverse GHG emissions trends (https://globalcarbonatlas.org/, last access: 1 March 2025), renders Cyprus a unique receptor

Deleted: As such, it stands as a strategic receptor site at the outflow of

Formatted: French (France)

Field Code Changed

Formatted: French (France)

Formatted: English (United States)

Formatted: English (United States)

site at the crossroads of continental outflows, making TCCON Nicosia strategically positioned for regional GHG monitoring.

Located in the EMME region, Cyprus is experiencing significant regional climate change (Ntoumos et al., 2020; Zittis et al., 2022). This has led to conditions, such as increased electricity demand for cooling, that contribute to higher GHG emissions (Gurriaran et al., 2023). Currently, the EMME region is poorly monitored for GHG concentration levels even though it holds nearly 60 % of the world's proven crude oil reserves (https://asb.opec.org/index.html, last access: 1 March 2025). This region is the third largest $CO_2$ emitter in the world and fourth for $CH_4$, with continuous fast-increasing GHG emissions, pointing out this region as a globally relevant GHG hotspot largely driven by the oil and gas sector (Bourtsoukidis et al., 2024; Germain-Piaulenne et al., 2024; Janssens-Maenhout et al., 2019; Paris et al., 2021).

Long-term GHG observation sites in the EMME region are scarce, primarily relying on ground-based in situ measurements, and have historically collected flask samples. These include the Weizmann Institute of Science in Israel (WIS) operational since 1995 (Lan, X. et al., 2024a, b, c; Petron, G. et al., 2024) and Finokalia (FKL), in Crete, Greece since 1993 (Gialesakis et al., 2023). The latter in situ GHG dataset reveals that while $CO_2$ levels reflect the general northern hemisphere (NH) growth rate (~2.5 $ppm \cdot y^{-1}$ since 2014), $CH_4$ levels are ~13 ppb higher than the NH average. The new data acquired at the TCCON site of Nicosia will provide a new insight into the balance of $CH_4$ regional sources and sinks being at the forefront to detect future changes in regional GHG emissions.

The aim of this paper is to a) describe the new TCCON Nicosia site and its setup, and b) present the first four (4) years of quality-controlled data from this new site. More specifically, Sect. 2 provides a description of the site characteristics and the experimental methods used. Section 3 presents the initial time series of selected retrieved gases, including a brief discussion on their temporal variability and a comparison with coincident AirCore measurements. Finally, Sect. 4 summarizes key findings and outlines directions for future work.

We note that the present study is intended as a technical site description and performance assessment study. Comprehensive analyses of the regional greenhouse-gas variability, air-mass origins, and transport mechanisms influencing the site will be addressed in forthcoming, dedicated scientific studies.

## 2 Methods

### 2.1 Site and instrumentation characteristics

#### 2.1.1 Location

Cyprus is the third largest island in the Mediterranean Sea (Fig. 1b); it spans approximately 240 km from east to west, and 100 km from north to south, with a population of approximately 1.36M inhabitants (https://worldpopulationreview.com/countries/cyprus-population, last access: 1 March 2025). It has a subtropical climate – Mediterranean and semi-arid type – with two main seasons; mild winters resembling spring (from December to March) and

Deleted: ; regions which currently exhibit diverse GHG emissions trends (https://globalcarbonatlas.org/, last access: 1 March 2025)

Deleted: section

Deleted: short

Deleted: along with

Deleted: results from AirCores

Deleted: section

warm-to-hot summers lasting about seven months (from April until October). Rainfall occurs primarily from November to April, with sunshine averaging from 160 to 400 hours per month (Michaelides et al., 2009; Pashiardis et al., 2017, 2023). These conditions are highly favorable for weather-dependent TCCON measurements that benefit from clear sky conditions. As such, the Nicosia site ensures excellent data coverage, among the highest within the TCCON, with approximately half the days of the year being sunny (i.e. < 20 % cloud cover) and less than 5 days per year being overcast (i.e. > 80 % cloud cover) (https://www.meteoblue.com/en/weather/historyclimate/climatemodelled/nicosia_cyprus_146268, last access: 1 March 2025).

The ground-based FTS station is owned by the University of Bremen (Germany) and was previously located at the GHG TCCON measurement site in Białystok, Poland (Messerschmidt et al., 2012). It was relocated in 2019 to The Cyprus Institute (CyI) premises in a residential area southeast of Nicosia (see Fig. 1c), 185 m above sea level (ASL) (Fig. 1d). The site is relatively close to Nicosia (~4 km from the city center), the largest city of the island (~400k inhabitants) with an elevation of ~150 m ASL (Fig. 1c). The city is located in the plain of Mesaoria bordered on its northern and southwestern sides by two mountain ranges, the Kyrenia Range (1024 m ASL), and the Troodos Mountains (1952 m ASL), respectively. This topography creates a NW-SE corridor that channels low-altitude winds (see Fig. 1b). This location also ensures that the line of sight of the solar-viewing instrument is unobstructed by local terrain, and can thus measure up to a solar zenith angle (SZA) of 85°.

The TCCON Nicosia measurements are an integral part of the Cyprus Atmospheric Observatory (https://cao.cyi.ac.cy/, last access: 1 March 2025). The CAO operates a network of stations across Cyprus, covering diverse atmospheric environments, including urban, regional background, free troposphere, and marine areas. This network provides extensive long-term datasets on atmospheric composition in the EMME (Baalbaki et al., 2021; Bimenyimana et al., 2023, 2025; Christodoulou et al., 2023; Dada et al., 2020; Deot et al., 2024; Kleanthous et al., 2014; Papetta et al., 2024; Pikridas et al., 2018; Vrekoussis et al., 2022; Yukhymchuk et al., 2022). The observatory integrates remote sensing (TCCON) and in situ techniques for comprehensive GHG monitoring, including ground-level GHG measurements on Cyprus's west coast at the remote village of Ineia, following the Integrated Carbon Observation System standards (ICOS; Heiskanen et al., 2022). It also supports aerosol and reactive gas monitoring under the European Aerosols, Clouds, and Trace Gases Research Infrastructure (ACTRIS, Laj et al., 2024).
These ground-based atmospheric monitoring facilities are completed by the Unmanned Systems Research Laboratory (https://usrl.cyi.ac.cy/, last access: 1 March 2025), a unique drone facility with a private airfield and airspace near the CAO regional background station. This enables in situ atmospheric profiling of key atmospheric species, including GHG, up to 6 km altitude (Kezoudi et al., 2020, 2021).

Deleted: shall

Deleted: Network

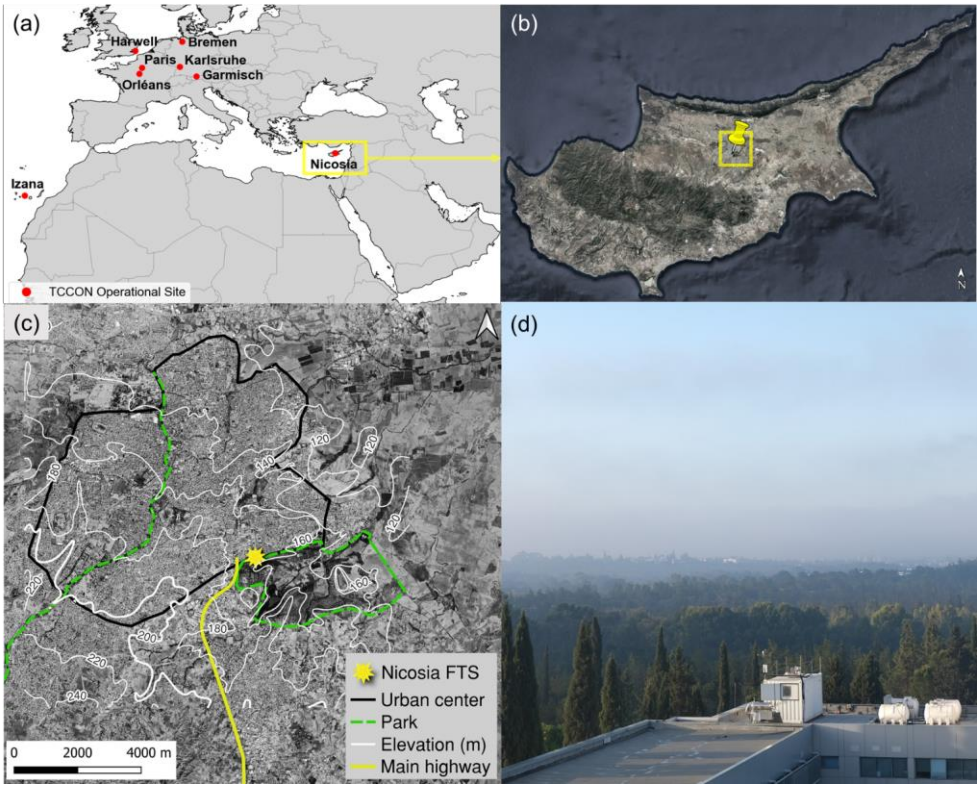


**Figure 1: (a) A zoom-in of the TCCON network map with European active site locations indicated with red solid circles. The yellow rectangle frame shows Cyprus. (b) Cyprus, and the city of Nicosia depicted by a yellow square; yellow pin denotes the Nicosia FTS. Map from Google Earth Pro, © 2025 Google LLC. (c) An elevation (solid white contours) map of the area around the Nicosia city center (delimited with a black line). Forested parks are represented by a dashed green line, the main highway in a solid yellow line and the FTS container is represented by a yellow sun. (d) The FTS container with a south view at the Nicosia site. The container is placed ~15 m above ground level, and the Athalassa National Forest Park is visible in the background.**

### 2.1.2 FTS instrument

The automated FTS system in Nicosia is based on a Bruker IFS 125HR spectrometer. A detailed overview of the system's setup and data acquisition is shown in Fig. 2 of Messerschmidt et al. (2012) with additional hardware details in the Appendix

of the same reference. Measurements began in September 2019, with the measurements configuration summarized in Table 1. The detectors setup is depicted and described in Fig. S1 in the supplementary material.

**[InGaAs detector (NIR)]:** The detector chamber employs an indium gallium arsenide **(**InGaAs) detector for near infrared (NIR) measurements in the 4000–11000 $cm^{-1}$ spectral region. The gas retrieval windows (TCCON) for this range are detailed in Laughner et al. (2024). Two types of measurements are conducted at Nicosia:

- High-resolution (NIR-HR) measurements performed at 64 cm Maximum Optical Path Difference (MOPD), and
- Low-resolution (NIR-LR) measurements at 1.8 cm MOPD, similar to the COCCON measurements (Frey et al., 2019).

The maximum optical path difference (MOPD) is set to 64 cm, consistent with the configuration used at the former site in Bialystok, Poland. This configuration exceeds the TCCON standard 45 cm, providing higher spectral resolution and thus making the spectra additionally valuable for independent spectroscopic trace-gas retrieval studies. In addition, the Nicosia site experiences relatively low cloud cover, so the slightly longer scan duration associated with the 64 cm MOPD does not significantly reduce data yield. The LR mode operates at a shorter scan time (~16.4 sec, at 10 kHz, for double-sided interferograms), compared to HR scans (~106 sec, at 10 kHz, for single-sided interferograms). Due to the shorter scan time, the LR data are particularly useful under partly cloudy conditions. The LR data, however, are stored separately from standard TCCON retrievals and are not included in the official TCCON products. These data can be retrieved using either the TCCON retrieval software (GGG, see Sect. 2.1.3), or PROFFAST, the official COCCON retrieval code (Alberti et al., 2022), providing more frequent measurements.

**[InSb detector]:** In December 2022, a liquid nitrogen–cooled indium antimonide detector ($LN_2$-InSb) was added to the Nicosia FTS, extending its sensitivity to the mid infrared (MIR; 1900 – 4200 $cm^{-1}$). The aim was to include Nicosia in the Network for the Detection of Atmospheric Composition Change (NDACC-IRWG, (De Mazière et al., 2018). High-resolution (0.005 $cm^{-1}$) solar absorption spectra recorded by NDACC FTIR spectrometers can provide precise documentation of multi-decadal trends of many tropospheric and stratospheric species, as well as insights into complex climate feedback processes (García et al., 2021; Vigouroux et al., 2015; Yamanouchi et al., 2023).

A 50/50 beam splitter ($CaF_2$, model BSW521 from THORLABS) is used which allows the MIR and NIR detectors to measure simultaneously (see Fig. S1 in supplement). This configuration uses five NDACC-IRWG band-pass filters (a-e) and one low-pass filter at 4200 $cm^{-1}$ (f) in front of the InSb detector, enabling the recording of additional spectra at the following wavenumber ranges: a) 1900 – 2230 $cm^{-1}$, b) 1970 – 2650 $cm^{-1}$, c) 2400 – 3200 $cm^{-1}$, d) 2900 – 3500 $cm^{-1}$, e) 3950 – 4200 $cm^{-1}$ and f) 1900 – 4200 $cm^{-1}$.

The MIR FTS technique enables the retrieval of several reactive gases in addition to the GHG, with the added potential of acquiring vertical information for a few of these species by exploiting the different retrieval sensitivity across the atmospheric layers (Buschmann et al., 2016; Chiarella et al., 2023; Zhou et al., 2019a, b).

**Table 1: Technical characteristics and observational capacity for TCCON Nicosia. Scanner speed at 0.32 cm·s$^{-1}$ (laser modulation frequency 10 kHz) from 01-09-2019 to 24-02-2024 – except for 01-12-2022 to 09-01-2023 where it was at 0.64 cm·s$^{-1}$ (20 kHz) – and 0.16 cm·s$^{-1}$ (5 kHz) from 07-02-2023 to 10-03-2023 and from 25-02-2024 after. Scanner speed was changed back to the TCCON standard at 0.32 cm.s$^{-1}$ (10 kHz) on 29-11-2024.**

| Measurement name | MOPD (cm) | Resolution (cm$^{-1}$) | Measuring detectors | Spectra wavenumber range (cm$^{-1}$) | Measured since (year) | Frequency |
|---|---|---|---|---|---|---|
| NIR (TCCON) | 64 | 0.016 | InGaAs | 4000 – 11000 (NIR) | 2019 | Daily |
| TCCON + MIR-1 | | | InGaAs + InSb | NIR, 1900 – 4200 | 2023 | Daily** |
| TCCON + MIR-2 | | | | NIR, 1900 – 2230 | | |
| TCCON + MIR-3 | | | | NIR, 1970 – 2230, 2400 – 2650 | | |
| TCCON + MIR-4 | | | | NIR, 2400 - 3200 | | |
| NIR-LR | 1.8 | 0.555 | InGaAs | NIR | 2019 | Daily |
| NIR-LR + low-pass | | | InGaAs + InSb | NIR, 1900 – 4200 | 2023 | Daily** |
| NDACC/IRWG (*) | 180 | 0.005 | InSb | 1900 – 2230 | 2023 | 2-3 times/week** |
| | | | | 1970 – 2230, 2400 – 2650 | | |
| | | | | 2400 – 3200 | | |
| | | | | 2900 – 3500 | | |
| | | | | 3950 – 4200 | | |

*With alternating sequence of filters. **When the InSb detector is $LN_2$-cooled.

### 2.1.3 FTS dataset

The official (public) data products $X_{CO_2}$, $X_{CH_4}$, $X_{CO}$, $X_{N_2O}$, $X_{HF}$, $X_{H_2O}$ and $X_{HDO}$ are retrieved with the latest TCCON Network retrieval software, the GGG2020 (Laughner et al., 2024). In short, the TCCON retrieval process used GEOS prior meteorology (GEOS FP-IT; (Lucchesi, 2015) before April 2024 and GEOS IT thereafter (https://gmao.gsfc.nasa.gov/GMAO_products/GEOS-IT/, last accessed 1 March 2025), and vertical profiles of atmospheric trace gases (priors) (Laughner et al., 2023) to simulate NIR solar absorption spectra. The latter are compared with the measured

spectra. From the best fit between the simulated and measured spectra, the vertical column abundances of trace gases ($VC_{gas}$, in molec.cm$^{-2}$) are retrieved, including that of oxygen ($VC_{O_2}$), a well-mixed gas with negligible relative variability. The DMF of a gas species ($X_{gas}$) is then defined as the ratio of the gas column ($VC_{gas}$) to the total column of air ($VC_{air}$):

$$X_{gas} = \frac{VC_{gas}}{VC_{air}} = 0.2095 \times \frac{VC_{gas}}{VC_{O_2}} \quad (1)$$

The use of this ratio not only cancels out spectroscopic effects common to both gas and $O_2$ columns, but also other systematic effects including alignment and pointing errors, while some spectroscopic uncertainties can partially cancel (see Appendix A(d) of Wunch et al. 2011 and Mendonca et al. 2019).

Deleted: errors

### 2.1.4 Data quality and performance checks

To ensure consistency across all the TCCON sites, standard quality diagnostic checks are implemented to identify potential instrumental-related issues affecting data precision. Here, we use $X_{luft}$ (the total column average of dry air), derived from surface pressure and the $O_2$ column ($VC_{O_2}$) retrieved within a ~250 cm$^{-1}$ window centered at 7885 cm$^{-1}$ (Mendonca et al., 2019), as a quality diagnostic indicator (Laughner et al., 2024).

Deleted: the retrieved

Deleted: near the

Formatted: Superscript

Deleted: line

Ideally, $X_{luft}$ should equal unity with a TCCON network nominal value of 0.999. Persistent deviations from the nominal $X_{luft}$ can indicate instrumental issues. Laughner et al. (2024) found that deviations from the network median correlate with biases in other $X_{gas}$ products, emphasizing the importance of maintaining a stable and close to nominal $X_{luft}$. Therefore, the standard TCCON quality control includes a check that $X_{luft}$ (after temporal smoothing) remains between 0.995 and 1.003, to keep these related biases within acceptable limits.

The TCCON Nicosia instrument experienced increased $X_{gas}$ and $X_{luft}$ variability due to a gradually loosening scanner electronic cable, present since installation in 2019 but identified and fixed only in November 2024. The issue led to longer scan durations and increased data spread, which became evident in 2022 when sufficient measurements were available. In parallel, the internal laser failed in April 2021, and its subsequent mis-focus after replacement reduced the number of valid scans, delaying the detection of the cable-related problem. During the affected period, we applied an empirical filter based on the $O_2$ line (7885 cm$^{-1}$) frequency shift ($O_2$_fs) to remove spectra outside the nominal $X_{luft}$ range before public data release. Applying the $O_2$_fs filter removed approximately 40 % of measurements, while most of the removed data lie within the 2022 period. Figure 2 shows the corrected $X_{luft}$ time series. Upcoming GGG2020 releases aim to address $X_{luft}$-correlated $X_{CO_2}$ biases (Laughner et al., 2024), potentially restoring the filtered data. The underlying issue causing the longer scan durations has since been resolved and no further occurrences have been observed after late 2024.

Deleted: In 2022, the TCCON Nicosia encountered unusual $X_{gas}$ and $X_{luft}$ spread due to a hardware issue (loose scanner electronic cable connection) that, since 22 November 2024, has been resolved. For the affected period, we applied an empirical filter on the $O_2$ line (7885 cm$^{-1}$) frequency shift ($O_2$_fs) values to exclude measurements falling outside the nominal $X_{luft}$ range before public data release. The recorded $O_2$_fs fluctuations occurred with refocusing or replacing the internal laser and were more pronounced from April 2021 to November 2022 due to poor laser focus; though this co-existed with the hardware issue since we identified affected spectra from 2019.

### 2.2 Evaluation of TCCON Nicosia against in situ vertical profiles (AirCores)

To tie the TCCON data to the World Meteorological Organization (WMO) reference scales (https://gml.noaa.gov/ccl/scales.html, last access: 1 March 2025) and to evaluate potential biases on the FTS data, TCCON applies a network-common multiplicative correction factor (CF) to each gas product, except for $X_{CO}$, as part of a post-retrieval

data processing before public release. These CFs are derived from WMO-referenced airborne in situ profiling above the FTS stations (Deutscher et al., 2010; Geibel et al., 2012; Messerschmidt et al., 2011; Wunch et al., 2010).

In Cyprus, we have performed three (3) AirCore (AC) (Baier et al., 2023; Karion et al., 2010) flights on 19 June (flight 1), 29 June (flight 2), and 30 June (flight 3) 2020. These flights provided vertical profiles of $CO_2$, $CH_4$, and CO up to approximately 22 km altitude (see Sect. S2.1 in supplement), providing valuable in situ information that extends well into the stratosphere. Data from the second and third flight are included in the most recent TCCON (GGG2020) "in situ correction" ensemble (Laughner et al., 2024). Although the GGG2020-derived CFs already incorporate information from these profiles, their limited contribution to the overall in situ dataset (2 out of 67 and 40 profiles for $CO_2$ and $CH_4$, respectively) suggests that evaluating the Nicosia measurements against these AirCores remains meaningful. Because only three AirCore profiles were available, the comparison was limited to a consistency check and interpretation of observed differences. A quantitative derivation of new correction factors for Nicosia would not be statistically robust and is already handled at the network level within GGG2020.

To compare FTS $X_{gas}$ with vertically resolved mole-fractions, such as in situ profiles from balloons or aircraft (or even model profiles), we compute a column integrated value directly from the in situ profile (here, the AirCore) using the Rodgers and Connor (2003) equation as adapted by Wunch et al. (2010) (Eq. 2):

$$C_s = \gamma C_a + \boldsymbol{\alpha}^T(x - \gamma x_a) \quad (2).$$

Here, $C_s$ is the column-averaged DMF, from hereafter the "AC.$X_{gas}$", $C_a$ is the column-averaged DMF from integrating the prior, $\gamma$ is the retrieval scaling factor, x and $x_a$ are the in situ-measured (true) and the prior (model) profile respectively, and $\boldsymbol{\alpha}$ is an element-wise product of the TCCON column averaging kernel $\mathbf{k}$ and a pressure-weighting function (see also Eq. 9-11, Sect. 8.3.1 of Laughner et al., 2024). The retrieval scaling factor quantifies the ratio of the retrieved to the prior column abundance. Both the retrieved and prior column averages are provided within the public TCCON data (i.e. 'xgas' and 'prior_xgas').

The TCCON wiki (https://tccon-wiki.caltech.edu/Main/AuxiliaryDataGGG2020, last access 1 March 2025) describes two methods for calculating comparison quantities, using "pressure weights" and using the "integration operator"; both methods have been applied and yield comparable results. The results presented here are obtained using the "pressure weights" method.

In this study, the comparison pair corresponds to public.$X_{gas}$ (the median of measurements within ±1 hour window around the AirCore flights' central time) and AC.$X_{gas}$, the AirCore-derived column after application of the TCCON averaging kernel (k) (see Eq.2). The public $X_{gas}$ data, entail uncertainties from a) imperfect spectroscopy and b) imperfect (wrong shape) priors. Applying the averaging kernel reduces the smoothing component of the uncertainty, such that the smoothing uncertainty becomes negligible for the comparison (see Laughner et al. (2024) and Wunch et al. (2010)). In order to disentangle uncertainties of type (a) from (b), we run the GGG2020 retrievals on TCCON spectra using the AirCore profiles (true profile shape) as the priors – i.e. a "custom retrieval" – which yields a "custom" $X_{gas}$ (custom.$X_{gas}$) (see also Sect. S2.5 in supplement).

**Deleted:** This evaluation exercise is only visual, and does not aim to derive new CF values for Nicosia.

**Deleted:** these

**Deleted:** quantities

**Deleted:** Here, t

**Deleted:** derived from

**Deleted:** T

**Deleted:** quantity

**Deleted:** AC.$X_{gas}$ is compared with the median value of the official TCCON $X_{gas}$ (i.e., public.$X_{gas}$) of the

**Formatted:** Subscript

**Deleted:** central time of each

**Formatted:** Subscript

**Deleted:** .¶
Differences amongst these two quantities will be due to the difference in the measurement principle ("remote sensing" versus "in situ") and their respective errors.

**Deleted:** .

**Deleted:** errors

**Deleted:** error

Both public and custom $X_{gas}$ data in this study include the Network-wide in situ correction, i.e. the airmass-independent correction factors (AICF; see Laughner et al., 2024).

Details on constructing the full in situ profiles (x) (Sect. S2.3-S2.4), selecting FTS data (Sect. S2.2) and the derivation and quantification of the individual uncertainties comprising the empirical total uncertainties for the compared quantities (public.$X_{gas}$ and AC.$X_{gas}$) (Sect. S2.6) are detailed in the supplementary material, following a similar – but not identical – approach as Laughner et al. (2024).

Deleted: associated

Deleted: Sect. S2.3-S2.6 in

## 3. Results

A brief overview of the TCCON-Nicosia database acquired up to the end of 2023 is provided in the following, starting with instrument performance, followed by a 4-year $X_{gas}$ time series, and concluding with a comparison of Nicosia $X_{gas}$ with data derived from the in situ profiles (AirCores).

### 3.1 Instrument performance

Figure 2 shows the $X_{luft}$ time series after applying the $O_2$_fs filtering, with metrics that can be used to assess the performance of the FTS, and provide an overview of the amount of valid TCCON data. After applying the $O_2$_fs filtering, the $X_{luft}$ 500-spectra running median (500-RMd) remains within the TCCON nominal values (0.995-1.003). Nicosia has approximately 1240 days of measurements from 1 September 2019 to 31 December 2023, with missing data due to weather conditions and instrument failures (e.g. broken laser, solar-tracker failure, maintenance and testing). The filtering approach reduced the amount of collected spectra by approximately 40% for the period impacted by the mentioned hardware issue. During the longest days of the year, and under clear-sky conditions, the Nicosia FTS has recorded up to 290 TCCON measurements.

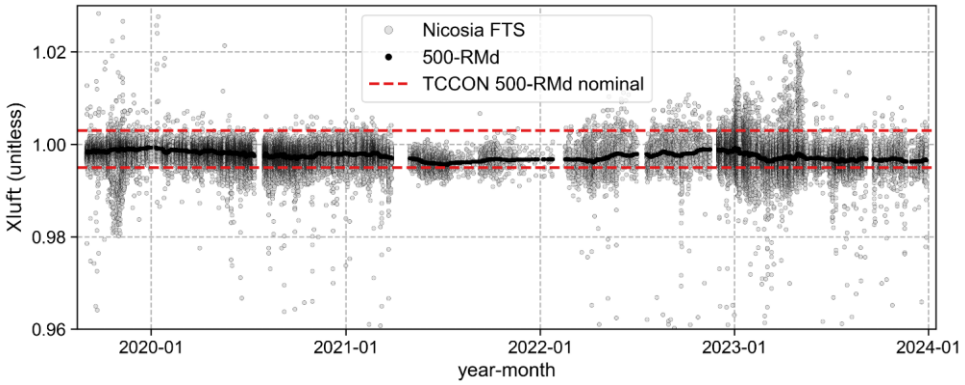


**Figure 2: $X_{luft}$ values after filtering out problematic data. Dashed red lines indicate the nominal values of 0.995 – 1.003 for the 500-spectra running median (500-RMd) (black line).**

### 3.2 Total column gases ($X_{gases}$) over Cyprus

This section presents the first publicly available columnar time series for the TCCON Nicosia site (and by extension over the EMME region) in the TCCON data repository, covering $X_{CO_2}$, $X_{CH_4}$ and $X_{CO}$. A brief discussion of the observed temporal behavior of the aforementioned $X_{gases}$ can be found below. A more extensive analysis of the temporal variability of these gases with back-trajectories and source attribution will be presented in follow-up studies.

#### 3.2.1 $X_{CO_2}$

Figure 3a shows that the $X_{CO_2}$ time series over Cyprus exhibits a pronounced seasonal cycle consistent with other Northern Hemisphere sites (Keppel-Aleks et al., 2011). The annual minimum occurs between August and September, while the maximum is observed between April and May, reflecting the dynamics of $CO_2$ sources and sinks that are primarily controlled by the seasonal cycles of photosynthesis and respiration (Randerson et al., 1997; Schimel, 1995). The overall increase over the years, driven by accumulation due to fossil fuel emissions (Keeling and Graven, 2021), occurs at a rate of 2.33±0.80 ppm·$y^{-1}$ between 2020 and 2023, which is slightly below the reported 2.5 ppm·$year^{-1}$ value obtained from ground-based observations performed in Crete (Greece) since 2014 (Gialesakis et al., 2023).

#### 3.2.2 $X_{CH_4}$

Figure 3b shows the time series of $X_{CH_4}$ at the TCCON-Nicosia site. Besides an overall continuous increase over the 4-year measurement period, a seasonal cycle can also be seen with minima observed between February and June. The maximum

Deleted: ¶
¶
¶

levels of $X_{CH_4}$ occur during the second half of the year, from July to December, with notable peaks in December and during the July-to-August period.

The July-August peaks over Cyprus could be explained by a combination of the following factors:

- The forest fire season over the Mediterranean region, as evidenced by a simultaneous increase in $X_{CO}$ (as a tracer of incomplete combustion) during the same period.
- Changes in the stratospheric amount of $CH_4$, driven by fluctuations in tropopause altitude (Washenfelder et al., 2003).

In addition, $X_{CH_4}$ exhibits a step-wise increase in the second half of each year – most notably in 2021 (see also Sect. 3.2.3) – which could be attributed to intense summer forest fire events. Moreover, transported regional pollution, originating from the Middle East sectors, which typically occurs during the fall and winter months (Kleanthous et al., 2014; Pikridas et al., 2018) may also contribute to this enhancement.

A minor peak of $X_{CH_4}$ in Fig. 3b is observed around mid-spring, most evident in spring 2020, which is likely associated with agricultural waste burning in Eastern Europe (Amiridis et al., 2010; Korontzi et al., 2006; Sciare et al., 2008; Stohl et al., 2007). A concurrent peak in $X_{CO}$ (Fig. 3c) during this period corroborates this link.

Deleted:

### 3.2.3 $X_{CO}$

Total column carbon monoxide does not exhibit any significant year-to-year trend. In contrast to $X_{CH_4}$, $X_{CO}$ shows an opposite seasonality pattern (Fig. 3c), with a minimum observed during the second half of the year, from June to December, and a maximum during the first half, from January to May. As noted earlier, peaks in July-August coincide with the forest fires season in the Mediterranean (Eke et al., 2024; Kaskaoutis et al., 2024; Masoom et al., 2023), during which $X_{CO}$ hourly values at our site exceeded 120 ppb. Due to the prolonged fires period in 2021, the mean $X_{CO}$ (95.2 ± 5.9 ppb) was higher than the adjacent years; 91.3 ± 5.2 ppb in 2020 and 87.9 ± 6.8 ppb in 2022.

Aside from wildfire events, CO levels in the troposphere of the EMME region are significantly influenced by fossil fuel combustion. Lelieveld et al. (2002) estimated that 60-80 % of the CO amount in the Mediterranean had originated from fossil fuel combustion in Western and Eastern Europe during the Mediterranean Intensive Oxidant Study (MINOS), performed in the summer of 2001.

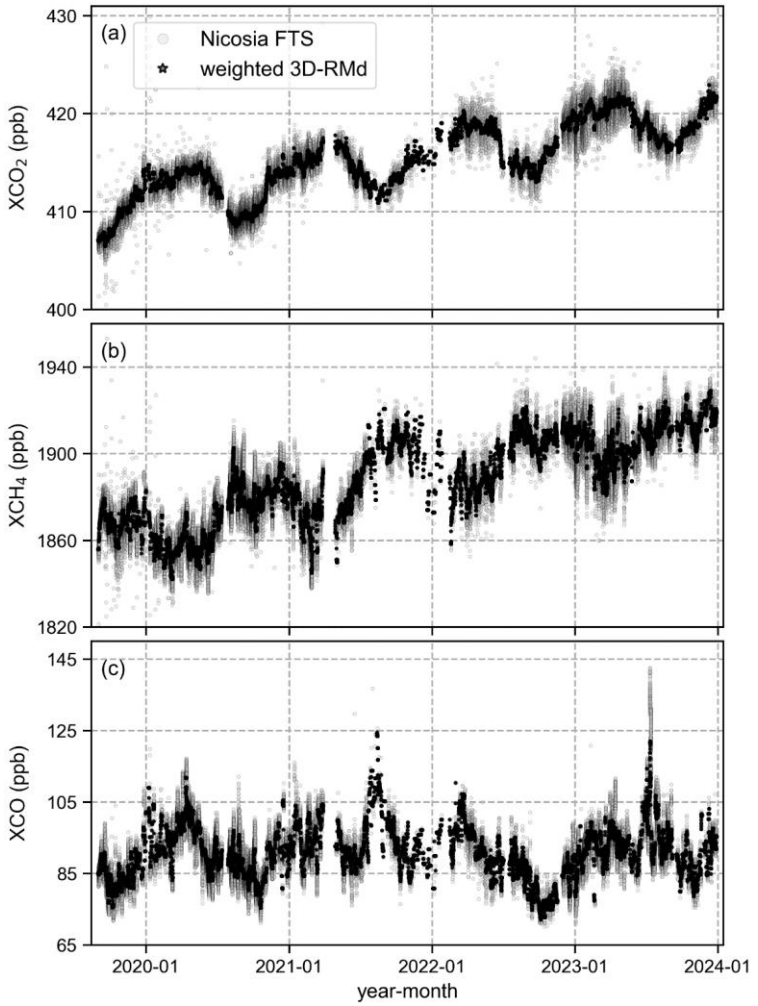


**Figure 3: The total columns of carbon dioxide ($X_{CO_2}$, (a)), methane ($X_{CH_4}$, (b)) and carbon monoxide ($X_{CO}$, (c)) from TCCON Nicosia. Grey markers represent FTS measurements, and black stars represent a 3-day running median, calculated from hourly means weighted by the squared inverse measurement error.**

### 3.3 TCCON Nicosia and AirCore comparison

This section describes a quantitative comparison between TCCON Nicosia public.$X_{gas}$ data and AirCore-derived total column quantities (AC.$X_{gas}$), aiming to evaluate the GGG2020 retrievals at Nicosia relative to the specific WMO-tied measurements (the Cyprus AirCores, June 2020).

#### 3.3.1 AirCore profiles

Figure 4 shows the in situ profiles obtained by the three AirCores sampled between 19 and 30 June 2020. These profiles reveal that the mole fraction of $CO_2$ has a relatively uniform vertical distribution with variations at the order of ~ 4 % between the surface and 20 km altitude. In contrast, $CH_4$ shows a mole fraction reduction of approximately 40% above 20 km altitude and CO of around 80 % over the same altitude range, compared to the ground.

During the flights of the June 29 and 30, a significant enhancement (+30 ppb) in the CO profiles (see Fig. 4c, grey and light-grey) was observed between the 12 – 17 km altitudes, along with smaller but still noticeable increases in $CH_4$ and $CO_2$ within the same altitude range. A HYSPLIT back-trajectory analysis (see Fig. S4 in supplement) was used to trace back the origin of air masses at these altitudes. These air masses were shown to originate from Southeast Asia and were transported to the Eastern Mediterranean via the Asian Summer Monsoon Anticyclone (ASMA) (Basha et al., 2020; Pan et al., 2016; Park et al., 2007; Santee et al., 2017). This annual meteorological phenomenon occurs annually, typically between 50° – 120° E, and is strongest near the Northern Hemisphere sub-tropical latitudes (Yihui and Chan, 2005). Under specific climatological conditions such as the approach of the Azores high on the western end of the Mediterranean causing a westward shift of the Monsoon low (Yadav, 2021), this phenomenon can affect the air quality of the Eastern Mediterranean region typically from the end of June to mid-August (Lawrence and Lelieveld, 2010; Lelieveld et al., 2001, 2002, 2018; Scheeren et al., 2003; Tyrlis et al., 2013).

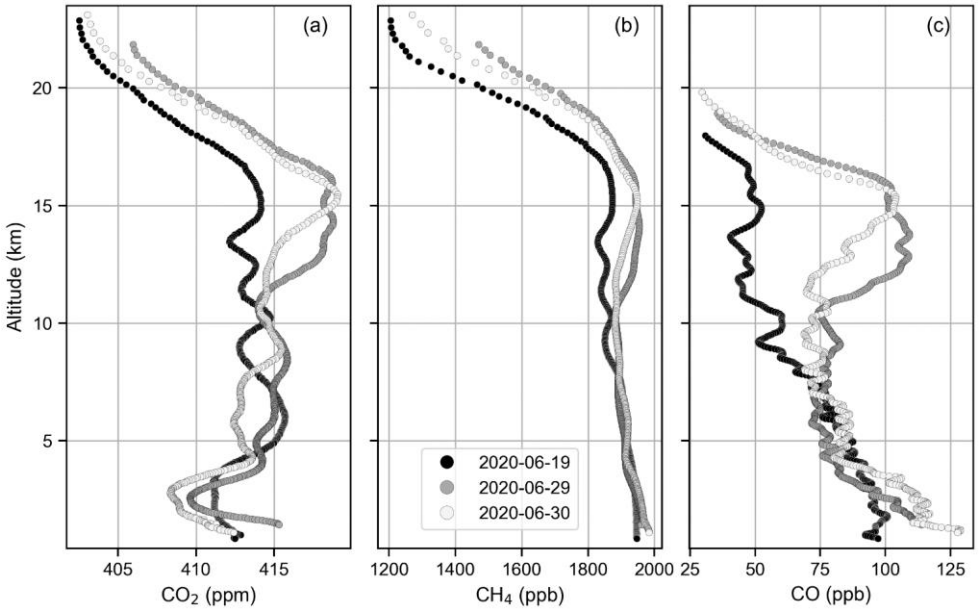


**Figure 4: The Nicosia, Cyprus AirCores; flights on June 19, 29, and 30 June 2020 in black, grey, and light grey, respectively. (a) Carbon dioxide, (b) methane and (c) carbon monoxide vertical profile. We apply an upper cutoff between 18 and 20 km altitude on the carbon monoxide CO profiles to remove non-real enhancements due to stratospheric ozone reactions inside the AirCore tubing.**

### 3.3.2 TCCON Nicosia Vs AirCore-derived data

TCCON Nicosia official data, public.$X_{gas}$, are compared with total column-integrated in situ measurements, AC.$X_{gas}$, to evaluate the consistency of TCCON Nicosia observations with its own (site specific) AirCores. Figure 5 shows the Nicosia AC.$X_{gas}$ in blue diamonds along with GGG2020 retrieved public data (grey circles and black line as the median). The custom.$X_{gas}$ value (dashed red line as the median of custom retrievals) (see Sect. 2.2) help assess the influence of trace gas prior profiles, used in simulating the NIR spectra, on TCCON retrievals. Consequently, any remaining differences may be date- (flight-), or site-specific originating from uncertainties in spectroscopy or instrument-related errors (see Sect. 9 and Fig. 23 of Laughner et al., 2024).

Table 2 summarizes these results for each gas species and flight. It shows the flight medians for both the public and custom retrieved $X_{gas}$ data, the integrated in situ $X_{gas}$ (AC.$X_{gas}$). These results show that the TCCON and the in situ AC.$X_{gas}$ agree within their calculated uncertainties range.

**Deleted:** , in a visual-only comparison

**Deleted:** , both standard

**Deleted:** public.$X_{gas}$,

**Deleted:** and custom retrievals (custom.$X_{gas}$, red stars)

**Deleted:** data

Since we quantify each uncertainty source separately (see Sect. S2.6 in supplementary material), we find that stratospheric uncertainty due to the un-sampled stratosphere, is typically the largest contributor to AC.$X_{CH_4}$ uncertainties (see Table S4, supplement). This is expected for methane, given its sharp decrease in the stratosphere. For AC.$X_{CH_4}$, the AC measurement uncertainty is the second most significant source and depends on the instrumentation – specifically, the AC sampler's resolution and the gas analyzer's precision.

For the AC.$X_{CO}$, the AC measurement uncertainty is the dominant source of uncertainty. This is primarily due to the gas analyzer's low precision for CO measurements, the low resolution of this specific AC sampler compared to a high-resolution AC (Membrive et al., 2017) and the stronger diffusion of carbon monoxide inside the AC tubing (Massman, 1998).

It is important to highlight that the GGG2020 $X_{CO}$ product, as discussed by Laughner et al. (2024), is not tied to a reference scale. Instead, its difference is assessed against in situ-derived data.

Laughner et al. (2024) in their Fig. 16 (e) show that, even though the $X_{CO}$ network mean difference across all the TCCON/in situ comparisons is small (~0.85 %), there is substantial variability in the TCCON/in situ $X_{CO}$ agreement, with individual measurements often exhibiting large uncertainties, with differences with respect to the in situ data up to ~30 %.

Differences between $X_{gas}$ and AC.$X_{gas}$ can arise from multiple sources:

1) Gas prior assumptions in the retrievals. For example, a vertical shift in the gas prior or an enhancement in prior CO concentrations can introduce biases of up to 1.5% in $X_{CO}$ retrievals (Laughner et al., 2024). The custom retrievals help isolate this effect by replacing GGG2020 priors with AC profiles.

2) Spatial and temporal sampling mismatches. The AC lands at a different location from launch and measures from the highest altitude downward, sampling a gas profile that is neither vertical nor coincident with the FTS line of sight (see Fig. S3 in supplement). Therefore, discrepancies between the AirCore trajectory and FTS line of sight may contribute to observed differences, particularly in spatially heterogeneous conditions (see Sect. S2.7 in the supplement). For instance, if the AirCore follows a west-to-east trajectory along a concentration gradient while the FTS observes toward the south, spatial variations in sampled air masses can lead to differences.

3) Atmospheric heterogeneity and boundary layer dynamics: Flight 2 (29 June 2020) exemplifies these challenges. The AirCore captured a near-surface enhancement around 2 km altitude (see Fig. 4a, dark grey profile), while ground-based in situ measurements showed a concurrent drawdown in $CH_4$ and CO (see Fig. S9) due to a shift in wind direction from westerly to northerly around 08:00 UTC (see Fig. S11, S12 in Sect. S2.7). This difference is reflected in the large ground uncertainty ($\epsilon$-ground = 0.20 ppm for AC.$X_{CO_2}$ versus 0.02 ppm for other flights, see Table S4 in Sect. S2.6). Combined with geometric sampling differences (small solar zenith angle and eastward AC trajectory versus SSW-directed FTS line of sight; see Fig. S3), the two instruments likely sampled different air masses. The fact that custom retrievals do not improve agreement supports the spatial mismatch hypothesis rather than indicating site-related biases. Despite these complexities, all comparisons agree within their combined uncertainties, demonstrating the robustness of the TCCON Nicosia measurements. A detailed case study analysis is provided in Sect. S2.7 in the supplementary material.

Deleted: error
Deleted: error
Deleted: error
Deleted: error
Deleted: ¶
Deleted: gas
Deleted: and
Deleted: in air mass sampling
Deleted: Concerning 1), for example, a vertical shift in the gas prior or an enhancement in prior CO concentrations can introduce biases of up to 1.5% in $X_{CO}$ retrievals (Laughner et al., 2024). Concerning 2), t
Deleted: the
Deleted: ,
Deleted: it
Deleted: starting at
Deleted: towards
Deleted: the ground,
Deleted: of the spectrometer
Deleted: the
Deleted: gas
Deleted: along a north-to-
Deleted: line of sight
Formatted: Subscript

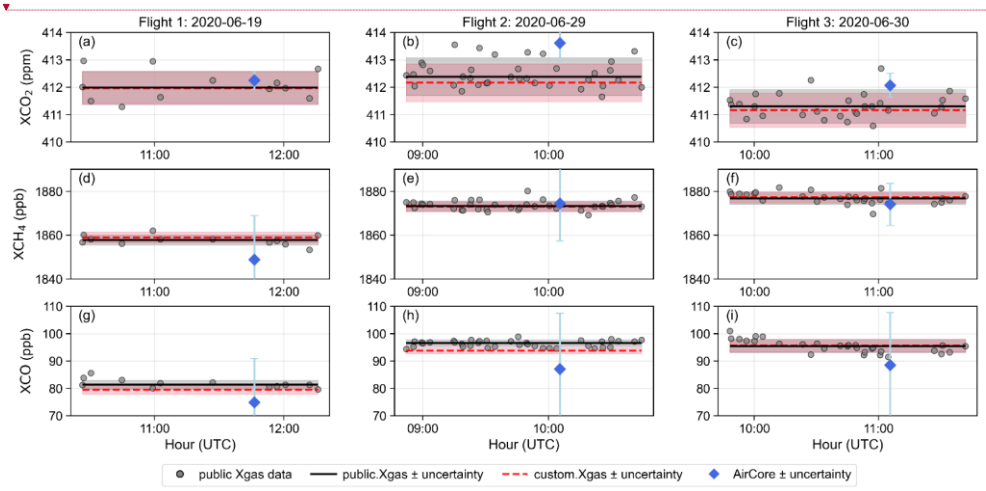


**Figure 5: Comparison of the Nicosia FTS data with the integrated in situ profiles. AirCore flights took place on the June, 19, 29 and 30 June 2020. The blue diamonds representing the AirCore total column are positioned at the AC landing time. Grey circles represent $XCO_2$ ((a)-(c)), $XCH_4$ ((d)-(f)) and XCO ((g)-(i)) Nicosia data versus time in hours (UTC) during the AirCore 'flight window' used for the comparison (±1 h around the AC central time). The black solid line represents the median of the $X_{gas}$ data and grey shaded area represents the total uncertainty (public.$X_{gas}$ ± uncertainty). Using the AirCore assembled profiles as trace gas priors in GGG2020, the custom retrieved data (custom $X_{gas}$) yield a corresponding median represented as a red dashed line and red shaded area represents the total uncertainty (custom.$X_{gas}$ ± uncertainty). The public and custom $X_{gas}$ uncertainty includes random effects caused by measurement variability and uncertainty caused by a not ideal $X_{luft}$. The AC.$X_{gas}$ uncertainty (blue uncertainty bars) include AC measurement uncertainty, stratospheric and ground uncertainty. For the detailed calculation of the uncertainty budget, refer to Sect. S2.6 in the supplementary material. Please note that some uncertainty bars in AC.$X_{gas}$ extend outside the y-axis limits.**

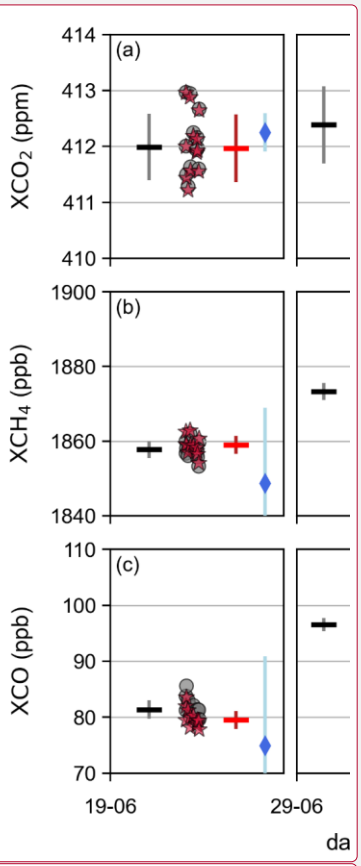


**Deleted:**

**Deleted:** (public.$X_{gas}$ ± error, black dash) …ith the integrated in situ profiles (AC.$X_{gas}$ ± error, blue diamonds)… AirCore flights took place on the June, 19, 29 and 30 June 2020. The blue diamonds representing the AirCore total column are positioned at the AC landing time. Grey circles represent $XCO_2$ ((a)-(c)), $XCH_4$ ((d)-(f)) and XCO ((g)-(i)) Nicosia data versus time in hours (UTC) during the AirCore 'flight window' used for the comparison (±1 h around the AC central time). For each gas, individual public data from the standard GGG2020 retrievals are shown as grey circles, while t…he black dash …

**Formatted:** Subscript

**Deleted:** error…. Using the AirCore assembled profiles as trace gas priors in GGG2020, the custom retrieved data (custom $X_{gas}$) are depicted by red stars, with the…ield a corresponding median represented as a red dashed line and red shaded area represents the total uncertainty (custom.$X_{gas}$ ± uncertaintyerror…. The public and custom $X_{gas}$ uncertainty error …ncludes the…random error …ffects caused by measurement variability and uncertaintydifferences…caused by a not ideal $X_{luft}$. The AC.$X_{gas}$ uncertaintyerror…(blue uncertaintyerror…bars) includes…AC measurement uncertainty, stratospheric and ground uncertaintyerror… For more details on …he detailed calculation of the uncertainty budgeterror analysis… refer to Sect. S2.B… in the supplementary material. Please note that some uncertaintyerr …

**Table 2: Retrieved and calculated $X_{gas}$ quantities. The public.Xgas (official Nicosia data) flight median ± total uncertainty value is compared to the AirCore derived comparison quantity (AC.$X_{gas}$ ± uncertainty). The custom retrieved Nicosia data (custom.$X_{gas}$ ± total uncertainty) (see Sect. 2.2 and S2.5 in supplement) are also shown here for comparison. The detailed uncertainty budget for all $X_{gas}$ products is presented in Sect. S2.6 in the supplementary material. Here, 'total uncertainty' denotes the combined uncertainty obtained by the reported random and known systematic contributions (see Sect. S2.6). Values are rounded to the nearest decimal.**

| Flight Number | 1 | 2 | 3 |
|---|---|---|---|
| | Quantity ± total uncertainty | | |
| AC.$X_{CO_2}$ (ppm) | 412.25 ± 0.35 | 413.61 ± 0.80 | 412.07 ± 0.45 |
| custom.$X_{CO_2}$ (ppm) | 411.96 ± 0.61 | 412.17 ± 0.69 | 411.16 ± 0.62 |
| public.$X_{CO_2}$ (ppm) | 411.99 ± 0.60 | 412.39 ± 0.69 | 411.30 ± 0.61 |
| AC.$X_{CH_4}$ (ppb) | 1848.7 ± 20.8 | 1874.4 ± 28.8 | 1874.1 ± 10.4 |
| custom.$X_{CH_4}$ (ppb) | 1859.0 ± 2.4 | 1872.9 ± 2.8 | 1877.3 ± 2.6 |
| public.$X_{CH_4}$ | 1857.8 ± 2.2 | 1873.3 ± 2.3 | 1876.7 ± 2.6 |
| AC.$X_{CO}$ (ppb) | 74.9 ± 17.1 | 87.1 ± 20.7 | 88.5 ± 19.5 |
| custom.$X_{CO}$ (ppb) | 79.5 ± 1.6 | 93.8 ± 1.1 | 95.7 ± 2.4 |
| public.$X_{CO}$ | 81.4 ± 1.6 | 96.6 ± 1.2 | 95.4 ± 2.3 |

Deleted: error
Deleted: error
Deleted: error
Deleted: B
Deleted: error
Deleted: values
Deleted: are discussed and calculated
Deleted: B6
Deleted: error
Deleted:

## 4. Conclusions and Outlook

The establishment of the ground-based FTS station in Nicosia, Cyprus – operational since September 2019 – represents a significant advancement in GHG monitoring for the Eastern Mediterranean and Middle East (EMME) region. This station is unique due to its geographical location at the crossroads of Europe, Asia, and Africa, providing critical observations in a climate-vulnerable region with complex atmospheric dynamics. The TCCON Nicosia setup includes two complementary measurement systems:

1. NIR solar absorption measurements (TCCON), providing total column observations of GHG, i.e. $X_{CO_2}$, $X_{CH_4}$, $X_{CO}$, $X_{N_2O}$, $X_{HF}$, $X_{H_2O}$ and $X_{HDO}$ since 2019. Future efforts will focus on extending $X_{gas}$ time series and continuously updating the public dataset. This will support long-term monitoring of seasonal and interannual trends and their relationship to climate variability in the EMME region.

2. MIR observations (NDACC-compatible), measuring additional trace gases, including HCHO, OCS, $NO_2$ and $C_2H_6$, since 2023. Future research will investigate these species, which can provide valuable insights into atmospheric chemistry, pollutant transport, and interactions with biogenic and anthropogenic sources.

The combination of these techniques enhances the station's long-term atmospheric monitoring capabilities and enables multi-species analyses. Additionally, Nicosia's consistently clear skies facilitate high data coverage (>70%), allowing future studies to gain detailed insights into seasonal cycles, diel variations, and special atmospheric events such as pollution episodes and long-range transport. This will improve our understanding of short-term variability and source attribution.

Independent evaluation through WMO-traceable AirCore observations confirms agreement of in situ with TCCON measurements within their uncertainties. However, with only three AirCore profiles available at Nicosia, further measurements – sampling with a high-resolution AirCore device to reduce uncertainties – at different time periods are needed to robustly assess the representativeness of these measurements.

The establishment of a ground-level GHG site on Cyprus's west coast (Ineia), compliant with ICOS recommendations, will provide valuable complementary measurements. The synergy between TCCON Nicosia total column data and Ineia in situ surface observations will offer a more comprehensive assessment of the atmospheric boundary layer and regional carbon budgets.

Future work will integrate TCCON Nicosia observations with atmospheric models to refine estimates of regional sources and sinks. This integration will provide insights to guide both regional and global climate policies aimed at reducing GHG concentrations.

In summary, the TCCON Nicosia station is a critical observational platform for monitoring GHGs in the EMME region. Its expanding measurement capabilities, ongoing improvements in data quality, and potential collaboration with in situ networks like ICOS will continue to provide valuable datasets supporting climate science and policy-driven mitigation efforts on both regional and global scales.

**Code availability**

The python code and ancillary data used for the AirCore analysis results presented in this paper are available online at: https://doi.org/10.5281/zenodo.15085719, last access 8 November 2025.

**Deleted:** 10.5281/zenodo.15085720

**Deleted:** 26

**Deleted:** March

**Data availability**

The Nicosia TCCON data can be accessed at https://data.caltech.edu/records/9kdk2-c5881, last access 5 December 2024.

The Cyprus AirCore data can be accessed at: https://zenodo.org/records/13132338, last access 5 December 2024.

The in situ ground data at the Nicosia location can be accessed at: https://doi.org/10.5281/zenodo.7788482, last access 5 December 2024.

**Supplement**

The supplement related to this article is available online at: https://doi.org/10.5281/zenodo.15085719, last access 8 November 2025.

Deleted: https://doi.org/10.5281/zenodo.15085720

Deleted: 26

Deleted: March

**Author contributions**

CR: Conceptualization, data curation, formal analysis, software, visualization, writing – original draft preparation, review & editing. CP: Data curation, formal analysis. PQ: Nicosia AirCore data sampling & analysis, software. TL: Nicosia AirCore profiles calculation, software. JL: Formal analysis, data curation, software, writing – review & editing. MD: Software, writing – review & editing. MP: Data curation, writing – review & editing. MR: Resources and AirCore profiles calculation. EB: Supervision, writing – review & editing. MB: Supervision, writing – review & editing. JN: Supervision, resources and funding acquisition, writing – review & editing. TW: Conceptualization, supervision, resources and funding acquisition, writing – review & editing. JP: Supervision, writing – review & editing. JS: Supervision, resources and funding acquisition, writing – review & editing. MV: Supervision, conceptualization, writing – review & editing.

**Competing interests**

At least one of the (co-)authors is a member of the editorial board of Atmospheric Measurement Techniques.

**Acknowledgements**

We acknowledge LSCE for providing the AirCore sampling system and for the profile calculation using the NOAA/GML code; we acknowledge Bianca Baier and Colm Sweeny for sharing this code. We acknowledge the Cyprus Department of Civil Aviation (DCA) for granting the permission to fly the AirCores. We thank the Air Navigation Services and the Airspace Management Cell (AMC) for the allocation of airspace and the procedures guide. Last, but not least, we thank the Nicosia Air Traffic Control and the Control Towers of Larnaca and Pafos Airports for the communication and support during the AirCore flights. We acknowledge Ms. Andreani Papageorgiou for creating the Nicosia elevation map in Fig. 1c.

**Financial support**

This publication has been produced within the framework of the EMME-CARE project, which received funding from the European Union's Horizon 2020 Research and Innovation Programme under grant agreement no. 856612 and from the Cyprus government, and the Edu4ClimAte project, which received funding from the European Commission's Horizon Europe Coordination & Support Action (CSA) "European Excellence Initiative" (EEI) programme under grant agreement no. 101071247. A portion of this research was carried out at the Jet Propulsion Laboratory (JPL), California Institute of Technology, under a contract with NASA (80NM0018D0004). USA Government sponsorship is acknowledged. Further support was provided by the University of Bremen, Germany.

**References**

Alberti, C., Hase, F., Frey, M., Dubravica, D., Blumenstock, T., Dehn, A., Castracane, P., Surawicz, G., Harig, R., Baier, B. C., Bès, C., Bi, J., Boesch, H., Butz, A., Cai, Z., Chen, J., Crowell, S. M., Deutscher, N. M., Ene, D., Franklin, J. E., García, O., Griffith, D., Grouiez, B., Grutter, M., Hamdouni, A., Houweling, S., Humpage, N., Jacobs, N., Jeong, S., Joly, L., Jones, N. B., Jouglet, D., Kivi, R., Kleinschek, R., Lopez, M., Medeiros, D. J., Morino, I., Mostafavipak, N., Müller, A., Ohyama, H., Palmer, P. I., Pathakoti, M., Pollard, D. F., Raffalski, U., Ramonet, M., Ramsay, R., Sha, M. K., Shiomi, K., Simpson, W., Stremme, W., Sun, Y., Tanimoto, H., Té, Y., Tsidu, G. M., Velazco, V. A., Vogel, F., Watanabe, M., Wei, C., Wunch, D., Yamasoe, M., Zhang, L., and Orphal, J.: Improved calibration procedures for the EM27/SUN spectrometers of the COllaborative Carbon Column Observing Network (COCCON), Atmospheric Meas. Tech., 15, 2433–2463, https://doi.org/10.5194/amt-15-2433-2022, 2022.

Amiridis, V., Giannakaki, E., Balis, D. S., Gerasopoulos, E., Pytharoulis, I., Zanis, P., Kazadzis, S., Melas, D., and Zerefos, C.: Smoke injection heights from agricultural burning in Eastern Europe as seen by CALIPSO, Atmospheric Chem. Phys., 10, 11567–11576, https://doi.org/10.5194/acp-10-11567-2010, 2010.

Baalbaki, R., Pikridas, M., Jokinen, T., Laurila, T., Dada, L., Bezantakos, S., Ahonen, L., Neitola, K., Maisser, A., Bimenyimana, E., Christodoulou, A., Unga, F., Savvides, C., Lehtipalo, K., Kangasluoma, J., Biskos, G., Petäjä, T., Kerminen, V.-M., Sciare, J., and Kulmala, M.: Towards understanding the characteristics of new particle formation in the Eastern Mediterranean, Atmospheric Chem. Phys., 21, 9223–9251, https://doi.org/10.5194/acp-21-9223-2021, 2021.

Babenhauserheide, A., Hase, F., and Morino, I.: Net $CO_2$ fossil fuel emissions of Tokyo estimated directly from measurements of the Tsukuba TCCON site and radiosondes, Atmospheric Meas. Tech., 13, 2697–2710, https://doi.org/10.5194/amt-13-2697-2020, 2020.

Baier, B. C., Sweeney, C., and Chen, H.: The AirCore atmospheric sampling system, in: Field Measurements for Passive Environmental Remote Sensing, Elsevier, 139–156, https://doi.org/10.1016/B978-0-12-823953-7.00014-9, 2023.

Basha, G., Ratnam, M. V., and Kishore, P.: Asian summer monsoon anticyclone: trends and variability, Atmospheric Chem. Phys., 20, 6789–6801, https://doi.org/10.5194/acp-20-6789-2020, 2020.

Bastos, A., O'Sullivan, M., Ciais, P., Makowski, D., Sitch, S., Friedlingstein, P., Chevallier, F., Rödenbeck, C., Pongratz, J., Luijkx, I. T., Patra, P. K., Peylin, P., Canadell, J. G., Lauerwald, R., Li, W., Smith, N. E., Peters, W., Goll, D. S., Jain, A. K., Kato, E., Lienert, S., Lombardozzi, D. L., Haverd, V., Nabel, J. E. M. S., Poulter, B., Tian, H., Walker, A. P., and Zaehle, S.:

Sources of Uncertainty in Regional and Global Terrestrial $CO_2$ Exchange Estimates, Glob. Biogeochem. Cycles, 34, e2019GB006393, https://doi.org/10.1029/2019GB006393, 2020.

Bimenyimana, E., Pikridas, M., Oikonomou, K., Iakovides, M., Christodoulou, A., Sciare, J., and Mihalopoulos, N.: Fine aerosol sources at an urban background site in the Eastern Mediterranean (Nicosia; Cyprus): Insights from offline versus online source apportionment comparison for carbonaceous aerosols, Sci. Total Environ., 893, 164741, https://doi.org/10.1016/j.scitotenv.2023.164741, 2023.

Bimenyimana, E., Sciare, J., Oikonomou, K., Iakovides, M., Pikridas, M., Vasiliadou, E., Savvides, C., and Mihalopoulos, N.: Cross-validation of methods for quantifying the contribution of local (urban) and regional sources to PM2.5 pollution: Application in the Eastern Mediterranean (Cyprus), Atmos. Environ., 343, 120975, https://doi.org/10.1016/j.atmosenv.2024.120975, 2025.

Bourtsoukidis, E., Germain-Piaulenne, E., Gros, V., Quéhé, P. -Y., Pikridas, M., Byron, J., Williams, J., Gliddon, D., Mohamed, R., Ekaabi, R., Lelieveld, J., Sciare, J., Teixidó, O., and Paris, J. -D.: Attribution of Excess Methane Emissions Over Marine Environments of the Mediterranean and Arabian Peninsula, J. Geophys. Res. Atmospheres, 129, e2024JD041621, https://doi.org/10.1029/2024JD041621, 2024.

Buschmann, M., Deutscher, N. M., Sherlock, V., Palm, M., Warneke, T., and Notholt, J.: Retrieval of $xCO_2$ from ground-based mid-infrared (NDACC) solar absorption spectra and comparison to TCCON, Atmospheric Meas. Tech., 9, 577–585, https://doi.org/10.5194/amt-9-577-2016, 2016.

Byrne, B., Baker, D. F., Basu, S., Bertolacci, M., Bowman, K. W., Carroll, D., Chatterjee, A., Chevallier, F., Ciais, P., Cressie, N., Crisp, D., Crowell, S., Deng, F., Deng, Z., Deutscher, N. M., Dubey, M. K., Feng, S., García, O. E., Griffith, D. W. T., Herkommer, B., Hu, L., Jacobson, A. R., Janardanan, R., Jeong, S., Johnson, M. S., Jones, D. B. A., Kivi, R., Liu, J., Liu, Z., Maksyutov, S., Miller, J. B., Miller, S. M., Morino, I., Notholt, J., Oda, T., O'Dell, C. W., Oh, Y.-S., Ohyama, H., Patra, P. K., Peiro, H., Petri, C., Philip, S., Pollard, D. F., Poulter, B., Remaud, M., Schuh, A., Sha, M. K., Shiomi, K., Strong, K., Sweeney, C., Té, Y., Tian, H., Velazco, V. A., Vrekoussis, M., Warneke, T., Worden, J. R., Wunch, D., Yao, Y., Yun, J., Zammit-Mangion, A., and Zeng, N.: National $CO_2$ budgets (2015–2020) inferred from atmospheric $CO_2$ observations in support of the global stocktake, Earth Syst. Sci. Data, 15, 963–1004, https://doi.org/10.5194/essd-15-963-2023, 2023.

Chiarella, R., Buschmann, M., Laughner, J., Morino, I., Notholt, J., Petri, C., Toon, G., Velazco, V. A., and Warneke, T.: A retrieval of $xCO_2$ from ground-based mid-infrared NDACC solar absorption spectra and comparison to TCCON, Atmospheric Meas. Tech., 16, 3987–4007, https://doi.org/10.5194/amt-16-3987-2023, 2023.

Christodoulou, A., Stavroulas, I., Vrekoussis, M., Desservettaz, M., Pikridas, M., Bimenyimana, E., Kushta, J., Ivančič, M., Rigler, M., Goloub, P., Oikonomou, K., Sarda-Estève, R., Savvides, C., Afif, C., Mihalopoulos, N., Sauvage, S., and Sciare, J.: Ambient carbonaceous aerosol levels in Cyprus and the role of pollution transport from the Middle East, Atmospheric Chem. Phys., 23, 6431–6456, https://doi.org/10.5194/acp-23-6431-2023, 2023.

Ciais, P., Dolman, A. J., Bombelli, A., Duren, R., Peregon, A., Rayner, P. J., Miller, C., Gobron, N., Kinderman, G., Marland, G., Gruber, N., Chevallier, F., Andres, R. J., Balsamo, G., Bopp, L., Bréon, F.-M., Broquet, G., Dargaville, R., Battin, T. J., Borges, A., Bovensmann, H., Buchwitz, M., Butler, J., Canadell, J. G., Cook, R. B., DeFries, R., Engelen, R., Gurney, K. R., Heinze, C., Heimann, M., Held, A., Henry, M., Law, B., Luyssaert, S., Miller, J., Moriyama, T., Moulin, C., Myneni, R. B., Nussli, C., Obersteiner, M., Ojima, D., Pan, Y., Paris, J.-D., Piao, S. L., Poulter, B., Plummer, S., Quegan, S., Raymond, P., Reichstein, M., Rivier, L., Sabine, C., Schimel, D., Tarasova, O., Valentini, R., Wang, R., Van Der Werf, G., Wickland, D., Williams, M., and Zehner, C.: Current systematic carbon-cycle observations and the need for implementing a policy-relevant carbon observing system, Biogeosciences, 11, 3547–3602, https://doi.org/10.5194/bg-11-3547-2014, 2014.

Dada, L., Ylivinkka, I., Baalbaki, R., Li, C., Guo, Y., Yan, C., Yao, L., Sarnela, N., Jokinen, T., Daellenbach, K. R., Yin, R., Deng, C., Chu, B., Nieminen, T., Wang, Y., Lin, Z., Thakur, R. C., Kontkanen, J., Stolzenburg, D., Sipilä, M., Hussein, T., Paasonen, P., Bianchi, F., Salma, I., Weidinger, T., Pikridas, M., Sciare, J., Jiang, J., Liu, Y., Petäjä, T., Kerminen, V.-M., and Kulmala, M.: Sources and sinks driving sulfuric acid concentrations in contrasting environments: implications on proxy calculations, Atmospheric Chem. Phys., 20, 11747–11766, https://doi.org/10.5194/acp-20-11747-2020, 2020.

De Mazière, M., Thompson, A. M., Kurylo, M. J., Wild, J. D., Bernhard, G., Blumenstock, T., Braathen, G. O., Hannigan, J. W., Lambert, J.-C., Leblanc, T., McGee, T. J., Nedoluha, G., Petropavlovskikh, I., Seckmeyer, G., Simon, P. C., Steinbrecht, W., and Strahan, S. E.: The Network for the Detection of Atmospheric Composition Change (NDACC): history, status and perspectives, Atmospheric Chem. Phys., 18, 4935–4964, https://doi.org/10.5194/acp-18-4935-2018, 2018.

Deng, Z., Ciais, P., Tzompa-Sosa, Z. A., Saunois, M., Qiu, C., Tan, C., Sun, T., Ke, P., Cui, Y., Tanaka, K., Lin, X., Thompson, R. L., Tian, H., Yao, Y., Huang, Y., Lauerwald, R., Jain, A. K., Xu, X., Bastos, A., Sitch, S., Palmer, P. I., Lauvaux, T., d'Aspremont, A., Giron, C., Benoit, A., Poulter, B., Chang, J., Petrescu, A. M. R., Davis, S. J., Liu, Z., Grassi, G., Albergel, C., Tubiello, F. N., Perugini, L., Peters, W., and Chevallier, F.: Comparing national greenhouse gas budgets reported in UNFCCC inventories against atmospheric inversions, Earth Syst. Sci. Data, 14, 1639–1675, https://doi.org/10.5194/essd-14-1639-2022, 2022.

Deot, N., Kanawade, V. P., Papetta, A., Baalbaki, R., Pikridas, M., Marenco, F., Kulmala, M., Sciare, J., Lehtipalo, K., and Jokinen, T.: Effect of planetary boundary layer evolution on new particle formation events over Cyprus, https://doi.org/10.5194/ar-2024-31, 24 October 2024.

Deutscher, N. M., Griffith, D. W. T., Bryant, G. W., Wennberg, P. O., Toon, G. C., Washenfelder, R. A., Keppel-Aleks, G., Wunch, D., Yavin, Y., Allen, N. T., Blavier, J.-F., Jiménez, R., Daube, B. C., Bright, A. V., Matross, D. M., Wofsy, S. C., and Park, S.: Total column $CO_2$ measurements at Darwin, Australia – site description and calibration against in situ aircraft profiles, Atmospheric Meas. Tech., 3, 947–958, https://doi.org/10.5194/amt-3-947-2010, 2010.

Eke, M., Cingiroglu, F., and Kaynak, B.: Investigation of 2021 wildfire impacts on air quality in southwestern Turkey, Atmos. Environ., 325, 120445, https://doi.org/10.1016/j.atmosenv.2024.120445, 2024.

European Environment Agency (EEA): https://www.eea.europa.eu/en/analysis/publications/annual-european-union-greenhouse-gas-inventory, last access 1 March 2025

Fraser, A., Palmer, P. I., Feng, L., Boesch, H., Cogan, A., Parker, R., Dlugokencky, E. J., Fraser, P. J., Krummel, P. B., Langenfelds, R. L., O'Doherty, S., Prinn, R. G., Steele, L. P., Van Der Schoot, M., and Weiss, R. F.: Estimating regional methane surface fluxes: the relative importance of surface and GOSAT mole fraction measurements, Atmospheric Chem. Phys., 13, 5697–5713, https://doi.org/10.5194/acp-13-5697-2013, 2013.

Frey, M., Sha, M. K., Hase, F., Kiel, M., Blumenstock, T., Harig, R., Surawicz, G., Deutscher, N. M., Shiomi, K., Franklin, J. E., Bösch, H., Chen, J., Grutter, M., Ohyama, H., Sun, Y., Butz, A., Mengistu Tsidu, G., Ene, D., Wunch, D., Cao, Z., Garcia, O., Ramonet, M., Vogel, F., and Orphal, J.: Building the COllaborative Carbon Column Observing Network (COCCON): long-term stability and ensemble performance of the EM27/SUN Fourier transform spectrometer, Atmospheric Meas. Tech., 12, 1513–1530, https://doi.org/10.5194/amt-12-1513-2019, 2019.

García, O. E., Schneider, M., Sepúlveda, E., Hase, F., Blumenstock, T., Cuevas, E., Ramos, R., Gross, J., Barthlott, S., Röhling, A. N., Sanromá, E., González, Y., Gómez-Peláez, Á. J., Navarro-Comas, M., Puentedura, O., Yela, M., Redondas, A., Carreño, V., León-Luis, S. F., Reyes, E., García, R. D., Rivas, P. P., Romero-Campos, P. M., Torres, C., Prats, N., Hernández, M., and López, C.: Twenty years of ground-based NDACC FTIR spectrometry at Izaña Observatory – overview and long-term comparison to other techniques, Atmospheric Chem. Phys., 21, 15519–15554, https://doi.org/10.5194/acp-21-15519-2021, 2021.

Geibel, M. C., Messerschmidt, J., Gerbig, C., Blumenstock, T., Chen, H., Hase, F., Kolle, O., Lavrič, J. V., Notholt, J., Palm, M., Rettinger, M., Schmidt, M., Sussmann, R., Warneke, T., and Feist, D. G.: Calibration of column-averaged $CH_4$ over European TCCON FTS sites with airborne in-situ measurements, Atmospheric Chem. Phys., 12, 8763–8775, https://doi.org/10.5194/acp-12-8763-2012, 2012.

Goddard Earth Observing System for Instrument Teams (GEOS-IT), https://gmao.gsfc.nasa.gov/GMAO_products/GEOS-IT/, last access 1 March 2025.

Germain-Piaulenne, E., Paris, J.-D., Gros, V., Quéhé, P.-Y., Pikridas, M., Baisnée, D., Berchet, A., Sciare, J., and Bourtsoukidis, E.: Middle East oil and gas methane emissions signature captured at a remote site using light hydrocarbon tracers, Atmospheric Environ. X, 22, 100253, https://doi.org/10.1016/j.aeaoa.2024.100253, 2024.

Gialesakis, N., Kalivitis, N., Kouvarakis, G., Ramonet, M., Lopez, M., Kwok, C. Y., Narbaud, C., Daskalakis, N., Mermigkas, M., Mihalopoulos, N., and Kanakidou, M.: A twenty year record of greenhouse gases in the Eastern Mediterranean atmosphere, Sci. Total Environ., 864, 161003, https://doi.org/10.1016/j.scitotenv.2022.161003, 2023.

Global Carbon Atlas: https://globalcarbonatlas.org/, last access 1 March 2025.

Gurriaran, L., Tanaka, K., Bayram, I. S., Proestos, Y., Lelieveld, J., and Ciais, P.: Warming-induced increase in power demand and CO2 emissions in Qatar and the Middle East, J. Clean. Prod., 382, 135359, https://doi.org/10.1016/j.jclepro.2022.135359, 2023.

Hedelius, J. K., Feng, S., Roehl, C. M., Wunch, D., Hillyard, P. W., Podolske, J. R., Iraci, L. T., Patarasuk, R., Rao, P., O'Keeffe, D., Gurney, K. R., Lauvaux, T., and Wennberg, P. O.: Emissions and topographic effects on column $CO_2$ ($X_{CO_2}$) variations, with a focus on the Southern California Megacity, J. Geophys. Res. Atmospheres, 122, 7200–7215, https://doi.org/10.1002/2017JD026455, 2017.

Heiskanen, J., Brümmer, C., Buchmann, N., Calfapietra, C., Chen, H., Gielen, B., Gkritzalis, T., Hammer, S., Hartman, S., Herbst, M., Janssens, I. A., Jordan, A., Juurola, E., Karstens, U., Kasurinen, V., Kruijt, B., Lankreijer, H., Levin, I., Linderson, M.-L., Loustau, D., Merbold, L., Myhre, C. L., Papale, D., Pavelka, M., Pilegaard, K., Ramonet, M., Rebmann, C., Rinne, J., Rivier, L., Saltikoff, E., Sanders, R., Steinbacher, M., Steinhoff, T., Watson, A., Vermeulen, A. T., Vesala, T., Vítková, G., and Kutsch, W.: The Integrated Carbon Observation System in Europe, Bull. Am. Meteorol. Soc., 103, E855–E872, https://doi.org/10.1175/BAMS-D-19-0364.1, 2022.

Janssens-Maenhout, G., Crippa, M., Guizzardi, D., Muntean, M., Schaaf, E., Dentener, F., Bergamaschi, P., Pagliari, V., Olivier, J. G. J., Peters, J. A. H. W., Van Aardenne, J. A., Monni, S., Doering, U., Petrescu, A. M. R., Solazzo, E., and Oreggioni, G. D.: EDGAR v4.3.2 Global Atlas of the three major greenhouse gas emissions for the period 1970–2012, Earth Syst. Sci. Data, 11, 959–1002, https://doi.org/10.5194/essd-11-959-2019, 2019.

Karion, A., Sweeney, C., Tans, P., and Newberger, T.: AirCore: An Innovative Atmospheric Sampling System, J. Atmospheric Ocean. Technol., 27, 1839–1853, https://doi.org/10.1175/2010JTECHA1448.1, 2010.

Kaskaoutis, D. G., Petrinoli, K., Grivas, G., Kalkavouras, P., Tsagkaraki, M., Tavernaraki, K., Papoutsidaki, K., Stavroulas, I., Paraskevopoulou, D., Bougiatioti, A., Liakakou, E., Rashki, A., Sotiropoulou, R. E. P., Tagaris, E., Gerasopoulos, E., and Mihalopoulos, N.: Impact of peri-urban forest fires on air quality and aerosol optical and chemical properties: The case of the August 2021 wildfires in Athens, Greece, Sci. Total Environ., 907, 168028, https://doi.org/10.1016/j.scitotenv.2023.168028, 2024.

Keeling, R. F. and Graven, H. D.: Insights from Time Series of Atmospheric Carbon Dioxide and Related Tracers, Annu. Rev. Environ. Resour., 46, 85–110, https://doi.org/10.1146/annurev-environ-012220-125406, 2021.

Keppel-Aleks, G., Wennberg, P. O., and Schneider, T.: Sources of variations in total column carbon dioxide, Atmospheric Chem. Phys., 11, 3581–3593, https://doi.org/10.5194/acp-11-3581-2011, 2011.

Keppel-Aleks, G., Wennberg, P. O., Washenfelder, R. A., Wunch, D., Schneider, T., Toon, G. C., Andres, R. J., Blavier, J.-F., Connor, B., Davis, K. J., Desai, A. R., Messerschmidt, J., Notholt, J., Roehl, C. M., Sherlock, V., Stephens, B. B., Vay, S. A., and Wofsy, S. C.: The imprint of surface fluxes and transport on variations in total column carbon dioxide, Biogeosciences, 9, 875–891, https://doi.org/10.5194/bg-9-875-2012, 2012.

Kezoudi, M., Tesche, M., Smith, H., Tsekeri, A., Baars, H., Dollner, M., Estellés, V., Weinzierl, B., Ulanowski, Z., Müller, D., and Amiridis, V.: Measurement report: Balloon-borne in-situ profiling of Saharan dust over Cyprus with the UCASS optical particle counter, https://doi.org/10.5194/acp-2020-977, 6 November 2020.

Kezoudi, M., Keleshis, C., Antoniou, P., Biskos, G., Bronz, M., Constantinides, C., Desservettaz, M., Gao, R.-S., Girdwood, J., Harnetiaux, J., Kandler, K., Leonidou, A., Liu, Y., Lelieveld, J., Marenco, F., Mihalopoulos, N., Močnik, G., Neitola, K., Paris, J.-D., Pikridas, M., Sarda-Esteve, R., Stopford, C., Unga, F., Vrekoussis, M., and Sciare, J.: The Unmanned Systems Research Laboratory (USRL): A New Facility for UAV-Based Atmospheric Observations, Atmosphere, 12, 1042, https://doi.org/10.3390/atmos12081042, 2021.

Kleanthous, S., Vrekoussis, M., Mihalopoulos, N., Kalabokas, P., and Lelieveld, J.: On the temporal and spatial variation of ozone in Cyprus, Sci. Total Environ., 476–477, 677–687, https://doi.org/10.1016/j.scitotenv.2013.12.101, 2014.

Korontzi, S., McCarty, J., Loboda, T., Kumar, S., and Justice, C.: Global distribution of agricultural fires in croplands from 3 years of Moderate Resolution Imaging Spectroradiometer (MODIS) data, Glob. Biogeochem. Cycles, 20, 2005GB002529, https://doi.org/10.1029/2005GB002529, 2006.

Laj, P., Lund Myhre, C., Riffault, V., Amiridis, V., Fuchs, H., Eleftheriadis, K., Petäjä, T., Salameh, T., Kivekäs, N., Juurola, E., Saponaro, G., Philippin, S., Cornacchia, C., Alados Arboledas, L., Baars, H., Claude, A., De Mazière, M., Dils, B., Dufresne, M., Evangeliou, N., Favez, O., Fiebig, M., Haeffelin, M., Herrmann, H., Höhler, K., Illmann, N., Kreuter, A., Ludewig, E., Marinou, E., Möhler, O., Mona, L., Eder Murberg, L., Nicolae, D., Novelli, A., O'Connor, E., Ohneiser, K., Petracca Altieri, R. M., Picquet-Varrault, B., Van Pinxteren, D., Pospichal, B., Putaud, J.-P., Reimann, S., Siomos, N., Stachlewska, I., Tillmann, R., Voudouri, K. A., Wandinger, U., Wiedensohler, A., Apituley, A., Comerón, A., Gysel-Beer, M., Mihalopoulos, N., Nikolova, N., Pietruczuk, A., Sauvage, S., Sciare, J., Skov, H., Svendby, T., Swietlicki, E., Tonev, D., Vaughan, G., Zdimal, V., Baltensperger, U., Doussin, J.-F., Kulmala, M., Pappalardo, G., Sorvari Sundet, S., and Vana, M.: Aerosol, Clouds and Trace Gases Research Infrastructure (ACTRIS): The European Research Infrastructure Supporting Atmospheric Science, Bull. Am. Meteorol. Soc., 105, E1098–E1136, https://doi.org/10.1175/BAMS-D-23-0064.1, 2024.

Lan, X., Mund, J.W., Crotwell, A.M., Thoning, K. W., Moglia, E., Madronich, M., Baugh, K., Petron, G., Crotwell, M.J., Neff, D., Wolter, S., Mefford, T., and DeVogel, S.: Atmospheric Carbon Dioxide Dry Air Mole Fractions from the NOAA GML Carbon Cycle Cooperative Global Air Sampling Network, 1968-2023, Version: 2024-07-30, 2024a.

Lan, X., Mund, J.W., Crotwell, A.M., Thoning, K. W., Moglia, E., Madronich, M., Baugh, K., Petron, G., Crotwell, M.J., Neff, D., Wolter, S., Mefford, T., and DeVogel, S.: Atmospheric Methane Dry Air Mole Fractions from the NOAA GML Carbon Cycle Cooperative Global Air Sampling Network, 1983-2023, Version: 2024-07-30, 2024b.

Lan, X., Mund, J.W., Crotwell, A.M., Thoning, K. W., Moglia, E., Madronich, M., Baugh, K., Petron, G., Crotwell, M.J., Neff, D., Wolter, S., Mefford, T., and DeVogel, S.: Atmospheric Nitrous Oxide Dry Air Mole Fractions from the NOAA GML Carbon Cycle Cooperative Global Air Sampling Network, 1997-2023, Version: 2024-07-30, 2024c.

Laughner, J. L., Roche, S., Kiel, M., Toon, G. C., Wunch, D., Baier, B. C., Biraud, S., Chen, H., Kivi, R., Laemmel, T., McKain, K., Quéhé, P.-Y., Rousogenous, C., Stephens, B. B., Walker, K., and Wennberg, P. O.: A new algorithm to generate

a priori trace gas profiles for the GGG2020 retrieval algorithm, Atmospheric Meas. Tech., 16, 1121–1146, https://doi.org/10.5194/amt-16-1121-2023, 2023.

Laughner, J. L., Toon, G. C., Mendonca, J., Petri, C., Roche, S., Wunch, D., Blavier, J.-F., Griffith, D. W. T., Heikkinen, P., Keeling, R. F., Kiel, M., Kivi, R., Roehl, C. M., Stephens, B. B., Baier, B. C., Chen, H., Choi, Y., Deutscher, N. M., DiGangi, J. P., Gross, J., Herkommer, B., Jeseck, P., Laemmel, T., Lan, X., McGee, E., McKain, K., Miller, J., Morino, I., Notholt, J., Ohyama, H., Pollard, D. F., Rettinger, M., Riris, H., Rousogenous, C., Sha, M. K., Shiomi, K., Strong, K., Sussmann, R., Té, Y., Velazco, V. A., Wofsy, S. C., Zhou, M., and Wennberg, P. O.: The Total Carbon Column Observing Network's GGG2020 data version, Earth Syst. Sci. Data, 16, 2197–2260, https://doi.org/10.5194/essd-16-2197-2024, 2024.

Lawrence, M. G. and Lelieveld, J.: Atmospheric pollutant outflow from southern Asia: a review, Atmospheric Chem. Phys., 10, 11017–11096, https://doi.org/10.5194/acp-10-11017-2010, 2010.

Lelieveld, J., Crutzen, P. J., Ramanathan, V., Andreae, M. O., Brenninkmeijer, C. A. M., Campos, T., Cass, G. R., Dickerson, R. R., Fischer, H., de Gouw, J. A., Hansel, A., Jefferson, A., Kley, D., Lawrence, M. G., Lobert, J. M., Mayol-Bracero, O. L., Mitra, A. P., Novakov, T., Oltmans, S. J., Prather, K. A., Reiner, T., Rodhe, H., Scheeren, H. A., Sikka, D., and Williams, J.: The Indian Ocean Experiment: Widespread Air Pollution from South and Southeast Asia, 291, 2001.

Lelieveld, J., Berresheim, H., Borrmann, S., Crutzen, P. J., Dentener, F. J., Fischer, H., Feichter, J., Flatau, P. J., Heland, J., Holzinger, R., Korrmann, R., Lawrence, M. G., Levin, Z., Markowicz, K. M., Mihalopoulos, N., Minikin, A., Ramanathan, V., De Reus, M., Roelofs, G. J., Scheeren, H. A., Sciare, J., Schlager, H., Schultz, M., Siegmund, P., Steil, B., Stephanou, E. G., Stier, P., Traub, M., Warneke, C., Williams, J., and Ziereis, H.: Global Air Pollution Crossroads over the Mediterranean, Science, 298, 794–799, https://doi.org/10.1126/science.1075457, 2002.

Lelieveld, J., Bourtsoukidis, E., Brühl, C., Fischer, H., Fuchs, H., Harder, H., Hofzumahaus, A., Holland, F., Marno, D., Neumaier, M., Pozzer, A., Schlager, H., Williams, J., Zahn, A., and Ziereis, H.: The South Asian monsoon—pollution pump and purifier, Science, 361, 270–273, https://doi.org/10.1126/science.aar2501, 2018.

Lucchesi, R.: File Specification for GEOS-5 FP-IT (forward processing for instrument teams), Tech. rep., NASA Goddard Space Flight Center, Greenbelt, MD, USA, 2015.

Masoom, A., Fountoulakis, I., Kazadzis, S., Raptis, I.-P., Kampouri, A., Psiloglou, B. E., Kouklaki, D., Papachristopoulou, K., Marinou, E., Solomos, S., Gialitaki, A., Founda, D., Salamalikis, V., Kaskaoutis, D., Kouremeti, N., Mihalopoulos, N., Amiridis, V., Kazantzidis, A., Papayannis, A., Zerefos, C. S., and Eleftheratos, K.: Investigation of the effects of the Greek extreme wildfires of August 2021 on air quality and spectral solar irradiance, Atmospheric Chem. Phys., 23, 8487–8514, https://doi.org/10.5194/acp-23-8487-2023, 2023.

Massman, W. J.: A review of the molecular diffusivities of $H_2O$, $CO_2$, $CH_4$, CO, $O_3$, $SO_2$, $NH_3$, $N_2O$, NO, and $NO_2$ in air, $O_2$ and $N_2$ near STP, Atmos. Environ., 32, 1111–1127, https://doi.org/10.1016/S1352-2310(97)00391-9, 1998.

Membrive, O., Crevoisier, C., Sweeney, C., Danis, F., Hertzog, A., Engel, A., Bönisch, H., and Picon, L.: AirCore-HR: a high-resolution column sampling to enhance the vertical description of $CH_4$ and $CO_2$, Atmospheric Meas. Tech., 10, 2163–2181, https://doi.org/10.5194/amt-10-2163-2017, 2017.

Mendonca, J., Strong, K., Wunch, D., Toon, G. C., Long, D. A., Hodges, J. T., Sironneau, V. T., and Franklin, J. E.: Using a speed-dependent Voigt line shape to retrieve $O_2$ from Total Carbon Column Observing Network solar spectra to improve measurements of $XCO_2$, Atmospheric Meas. Tech., 12, 35–50, https://doi.org/10.5194/amt-12-35-2019, 2019.

Messerschmidt, J., Geibel, M. C., Blumenstock, T., Chen, H., Deutscher, N. M., Engel, A., Feist, D. G., Gerbig, C., Gisi, M., Hase, F., Katrynski, K., Kolle, O., Lavrič, J. V., Notholt, J., Palm, M., Ramonet, M., Rettinger, M., Schmidt, M., Sussmann,

R., Toon, G. C., Truong, F., Warneke, T., Wennberg, P. O., Wunch, D., and Xueref-Remy, I.: Calibration of TCCON column-averaged $CO_2$: the first aircraft campaign over European TCCON sites, Atmospheric Chem. Phys., 11, 10765–10777, https://doi.org/10.5194/acp-11-10765-2011, 2011.

Messerschmidt, J., Chen, H., Deutscher, N. M., Gerbig, C., Grupe, P., Katrynski, K., Koch, F.-T., Lavrič, J. V., Notholt, J., Rödenbeck, C., Ruhe, W., Warneke, T., and Weinzierl, C.: Automated ground-based remote sensing measurements of greenhouse gases at the Białystok site in comparison with collocated in situ measurements and model data, Atmospheric Chem. Phys., 12, 6741–6755, https://doi.org/10.5194/acp-12-6741-2012, 2012.

Meteoblue, https://www.meteoblue.com/en/weather/historyclimate/climatemodelled/nicosia_cyprus_146268, last access 1 March 2025.

Michaelides, S. C., Tymvios, F. S., and Michaelidou, T.: Spatial and temporal characteristics of the annual rainfall frequency distribution in Cyprus, Atmospheric Res., 94, 606–615, https://doi.org/10.1016/j.atmosres.2009.04.008, 2009.

Ntoumos, A., Hadjinicolaou, P., Zittis, G., and Lelieveld, J.: Updated Assessment of Temperature Extremes over the Middle East–North Africa (MENA) Region from Observational and CMIP5 Data, Atmosphere, 11, 813, https://doi.org/10.3390/atmos11080813, 2020.

OPEC Annual Statistical Bulletin: https://publications.opec.org/asb, last access 1 March 2025.

Pan, L. L., Honomichl, S. B., Kinnison, D. E., Abalos, M., Randel, W. J., Bergman, J. W., and Bian, J.: Transport of chemical tracers from the boundary layer to stratosphere associated with the dynamics of the Asian summer monsoon, J. Geophys. Res. Atmospheres, 121, https://doi.org/10.1002/2016JD025616, 2016.

Papetta, A., Marenco, F., Kezoudi, M., Mamouri, R.-E., Nisantzi, A., Baars, H., Popovici, I. E., Goloub, P., Victori, S., and Sciare, J.: Lidar depolarization characterization using a reference system, Atmospheric Meas. Tech., 17, 1721–1738, https://doi.org/10.5194/amt-17-1721-2024, 2024.

Paris, J.-D., Riandet, A., Bourtsoukidis, E., Delmotte, M., Berchet, A., Williams, J., Ernle, L., Tadic, I., Harder, H., and Lelieveld, J.: Shipborne measurements of methane and carbon dioxide in the Middle East and Mediterranean areas and contribution from oil andgas emissions, https://doi.org/10.5194/acp-2021-114, 5 March 2021.

Park, M., Randel, W. J., Gettelman, A., Massie, S. T., and Jiang, J. H.: Transport above the Asian summer monsoon anticyclone inferred from Aura Microwave Limb Sounder tracers, J. Geophys. Res. Atmospheres, 112, 2006JD008294, https://doi.org/10.1029/2006JD008294, 2007.

Pashiardis, S., Kalogirou, S. A., and Pelengaris, A.: Statistical analysis for the characterization of solar energy utilization and inter-comparison of solar radiation at two sites in Cyprus, Appl. Energy, 190, 1138–1158, https://doi.org/10.1016/j.apenergy.2017.01.018, 2017.

Pashiardis, S., Pelengaris, A., and Kalogirou, S. A.: Geographical Distribution of Global Radiation and Sunshine Duration over the Island of Cyprus, Appl. Sci., 13, 5422, https://doi.org/10.3390/app13095422, 2023.

Petron, G., Crotwell, A.M., Madronich, M., Moglia, E., Baugh, K.E., Kitzis, D., Mefford, T., DeVogel, S., Neff, D., Lan, X., Crotwell, M.J., Thoning, K., Wolter, S., and Mund, J.W.: Atmospheric Carbon Monoxide Dry Air Mole Fractions from the NOAA GML Carbon Cycle Cooperative Global Air Sampling Network, 1988-2023, Version: 2024-07-30, 2024.

Pikridas, M., Vrekoussis, M., Sciare, J., Kleanthous, S., Vasiliadou, E., Kizas, C., Savvides, C., and Mihalopoulos, N.: Spatial and temporal (short and long-term) variability of submicron, fine and sub-10 μm particulate matter (PM1, PM2.5, PM10) in Cyprus, Atmos. Environ., 191, 79–93, https://doi.org/10.1016/j.atmosenv.2018.07.048, 2018.

Randerson, J. T., Thompson, M. V., Conway, T. J., Fung, I. Y., and Field, C. B.: The contribution of terrestrial sources and sinks to trends in the seasonal cycle of atmospheric carbon dioxide, Glob. Biogeochem. Cycles, 11, 535–560, https://doi.org/10.1029/97GB02268, 1997.

Rodgers, C. D. and Connor, B. J.: Intercomparison of remote sounding instruments, J. Geophys. Res. Atmospheres, 108, 2002JD002299, https://doi.org/10.1029/2002JD002299, 2003.

Rousogenous, C. (2025). Supplementary material for TCCON Nicosia site description manuscript. Zenodo. https://doi.org/10.5281/zenodo.15085719, last access 8 November 2025.

Santee, M. L., Manney, G. L., Livesey, N. J., Schwartz, M. J., Neu, J. L., and Read, W. G.: A comprehensive overview of the climatological composition of the Asian summer monsoon anticyclone based on 10 years of Aura Microwave Limb Sounder measurements, J. Geophys. Res. Atmospheres, 122, 5491–5514, https://doi.org/10.1002/2016JD026408, 2017.

Scheeren, H. A., Lelieveld, J., Roelofs, G. J., Williams, J., Fischer, H., de Reus, M., de Gouw, J. A., Warneke, C., Holzinger, R., and Schlager, H.: The impact of monsoon outflow from India and Southeast Asia in the upper troposphere over the eastern Mediterranean, Atmos Chem Phys, 2003.

Schimel, D., Pavlick, R., Fisher, J. B., Asner, G. P., Saatchi, S., Townsend, P., Miller, C., Frankenberg, C., Hibbard, K., and Cox, P.: Observing terrestrial ecosystems and the carbon cycle from space, Glob. Change Biol., 21, 1762–1776, https://doi.org/10.1111/gcb.12822, 2015.

Schimel, D. S.: Terrestrial ecosystems and the carbon cycle, Glob. Change Biol., 1, 77–91, https://doi.org/10.1111/j.1365-2486.1995.tb00008.x, 1995.

Sciare, J., Oikonomou, K., Favez, O., Liakakou, E., Markaki, Z., Cachier, H., and Mihalopoulos, N.: Long-term measurements of carbonaceous aerosols in the Eastern Mediterranean: evidence of long-range transport of biomass burning, Atmospheric Chem. Phys., 8, 5551–5563, https://doi.org/10.5194/acp-8-5551-2008, 2008.

Sha, M. K., Langerock, B., Blavier, J.-F. L., Blumenstock, T., Borsdorff, T., Buschmann, M., Dehn, A., De Mazière, M., Deutscher, N. M., Feist, D. G., García, O. E., Griffith, D. W. T., Grutter, M., Hannigan, J. W., Hase, F., Heikkinen, P., Hermans, C., Iraci, L. T., Jeseck, P., Jones, N., Kivi, R., Kumps, N., Landgraf, J., Lorente, A., Mahieu, E., Makarova, M. V., Mellqvist, J., Metzger, J.-M., Morino, I., Nagahama, T., Notholt, J., Ohyama, H., Ortega, I., Palm, M., Petri, C., Pollard, D. F., Rettinger, M., Robinson, J., Roche, S., Roehl, C. M., Röhling, A. N., Rousogenous, C., Schneider, M., Shiomi, K., Smale, D., Stremme, W., Strong, K., Sussmann, R., Té, Y., Uchino, O., Velazco, V. A., Vigouroux, C., Vrekoussis, M., Wang, P., Warneke, T., Wizenberg, T., Wunch, D., Yamanouchi, S., Yang, Y., and Zhou, M.: Validation of methane and carbon monoxide from Sentinel-5 Precursor using TCCON and NDACC-IRWG stations, Atmospheric Meas. Tech., 14, 6249–6304, https://doi.org/10.5194/amt-14-6249-2021, 2021.

Stohl, A., Berg, T., Burkhart, J. F., Fjæraa, A. M., Forster, C., Herber, A., Hov, Ø., Lunder, C., McMillan, W. W., Oltmans, S., Shiobara, M., Simpson, D., Solberg, S., Stebel, K., Ström, J., Tørseth, K., Treffeisen, R., Virkkunen, K., and Yttri, K. E.: Arctic smoke - record high air pollution levels in the European Arctic due to agricultural fires in Eastern Europe in spring 2006, Atmospheric Chem. Phys., 7, 511–534, https://doi.org/10.5194/acp-7-511-2007, 2007.

TCCON data, https://tccondata.org/, last access 1 March 2025.

**Deleted:** https://doi.org/10.5281/zenodo.15085720

**Deleted:** 26

**Deleted:** March

TCCON-wiki, https://tccon-wiki.caltech.edu/Main/AuxiliaryDataGGG2020, last access 1 March 2025.

Tyrlis, E., Lelieveld, J., and Steil, B.: The summer circulation over the eastern Mediterranean and the Middle East: influence of the South Asian monsoon, Clim. Dyn., 40, 1103–1123, https://doi.org/10.1007/s00382-012-1528-4, 2013.

Unmanned Systems Research Laboratory (USRL): https://usrl.cyi.ac.cy/, last access 1 March 1, 2025.

Vigouroux, C., Blumenstock, T., Coffey, M., Errera, Q., García, O., Jones, N. B., Hannigan, J. W., Hase, F., Liley, B., Mahieu, E., Mellqvist, J., Notholt, J., Palm, M., Persson, G., Schneider, M., Servais, C., Smale, D., Thölix, L., and De Mazière, M.: Trends of ozone total columns and vertical distribution from FTIR observations at eight NDACC stations around the globe, Atmospheric Chem. Phys., 15, 2915–2933, https://doi.org/10.5194/acp-15-2915-2015, 2015.

Vrekoussis, M., Pikridas, M., Rousogenous, C., Christodoulou, A., Desservettaz, M., Sciare, J., Richter, A., Bougoudis, I., Savvides, C., and Papadopoulos, C.: Local and regional air pollution characteristics in Cyprus: A long-term trace gases observations analysis, Sci. Total Environ., 845, 157315, https://doi.org/10.1016/j.scitotenv.2022.157315, 2022.

Washenfelder, R. A., Wennberg, P. O., and Toon, G. C.: Tropospheric methane retrieved from ground-based near-IR solar absorption spectra, Geophys. Res. Lett., 30, 2003GL017969, https://doi.org/10.1029/2003GL017969, 2003.

World Meteorological Organization (WMO) Central Calibration Laboratory (CCL): https://gml.noaa.gov/ccl/scales.html, last access 1 March 2025.

World Population Review, https://worldpopulationreview.com/countries/cyprus, last access 1 March 2025.

Wunch, D., Toon, G. C., Wennberg, P. O., Wofsy, S. C., Stephens, B. B., Fischer, M. L., Uchino, O., Abshire, J. B., Bernath, P., Biraud, S. C., Blavier, J. F. L., Boone, C., Bowman, K. P., Browell, E. V., Campos, T., Connor, B. J., Daube, B. C., Deutscher, N. M., Diao, M., Elkins, J. W., Gerbig, C., Gottlieb, E., Griffith, D. W. T., Hurst, D. F., Jiménez, R., Keppel-Aleks, G., Kort, E. A., MacAtangay, R., MacHida, T., Matsueda, H., Moore, F., Morino, I., Park, S., Robinson, J., Roehl, C. M., Sawa, Y., Sherlock, V., Sweeney, C., Tanaka, T., and Zondlo, M. A.: Calibration of the total carbon column observing network using aircraft profile data, Atmospheric Meas. Tech., 3, 1351–1362, https://doi.org/10.5194/amt-3-1351-2010, 2010.

Wunch, D., Toon, G. C., Blavier, J.-F. L., Washenfelder, R. A., Notholt, J., Connor, B. J., Griffith, D. W. T., Sherlock, V., and Wennberg, P. O.: The Total Carbon Column Observing Network, Philos. Trans. R. Soc. Math. Phys. Eng. Sci., 369, 2087–2112, https://doi.org/10.1098/rsta.2010.0240, 2011.

Yadav, R. K.: Relationship between Azores High and Indian summer monsoon, Npj Clim. Atmospheric Sci., 4, 26, https://doi.org/10.1038/s41612-021-00180-z, 2021.

Yamanouchi, S., Conway, S., Strong, K., Colebatch, O., Lutsch, E., Roche, S., Taylor, J., Whaley, C. H., and Wiacek, A.: Network for the Detection of Atmospheric Composition Change (NDACC) Fourier transform infrared (FTIR) trace gas measurements at the University of Toronto Atmospheric Observatory from 2002 to 2020, Earth Syst. Sci. Data, 15, 3387–3418, https://doi.org/10.5194/essd-15-3387-2023, 2023.

Yihui, D. and Chan, J. C. L.: The East Asian summer monsoon: an overview, Meteorol. Atmospheric Phys., 89, 117–142, https://doi.org/10.1007/s00703-005-0125-z, 2005.

Yukhymchuk, Y., Milinevsky, G., Syniavskyi, I., Popovici, I., Unga, F., Sciare, J., Marenco, F., Pikridas, M., and Goloub, P.: Atmospheric Aerosol Outbreak over Nicosia, Cyprus, in April 2019: Case Study, Atmosphere, 13, 1997, https://doi.org/10.3390/atmos13121997, 2022.

Zhou, M., Langerock, B., Wells, K. C., Millet, D. B., Vigouroux, C., Sha, M. K., Hermans, C., Metzger, J.-M., Kivi, R., Heikkinen, P., Smale, D., Pollard, D. F., Jones, N., Deutscher, N. M., Blumenstock, T., Schneider, M., Palm, M., Notholt, J., Hannigan, J. W., and De Mazière, M.: An intercomparison of total column-averaged nitrous oxide between ground-based FTIR TCCON and NDACC measurements at seven sites and comparisons with the GEOS-Chem model, Atmospheric Meas. Tech., 12, 1393–1408, https://doi.org/10.5194/amt-12-1393-2019, 2019a.

Zhou, M., Langerock, B., Sha, M. K., Kumps, N., Hermans, C., Petri, C., Warneke, T., Chen, H., Metzger, J.-M., Kivi, R., Heikkinen, P., Ramonet, M., and De Mazière, M.: Retrieval of atmospheric $CH_4$ vertical information from ground-based FTS near-infrared spectra, Atmospheric Meas. Tech., 12, 6125–6141, https://doi.org/10.5194/amt-12-6125-2019, 2019b.

Zittis, G., Almazroui, M., Alpert, P., Ciais, P., Cramer, W., Dahdal, Y., Fnais, M., Francis, D., Hadjinicolaou, P., Howari, F., Jrrar, A., Kaskaoutis, D. G., Kulmala, M., Lazoglou, G., Mihalopoulos, N., Lin, X., Rudich, Y., Sciare, J., Stenchikov, G., Xoplaki, E., and Lelieveld, J.: Climate Change and Weather Extremes in the Eastern Mediterranean and Middle East, Rev. Geophys., 60, e2021RG000762, https://doi.org/10.1029/2021RG000762, 2022.